1969

Some aspects of aerated open-channel flow at shallow depths and low velocities

D. L. Fread

SOME ASPECTS OF AERATED OPEN-CHANNEL FLOW AT SHALLOW DEPTHS AND LOW VELOCITIES

BY

DANNY LEE FREAD, 1938-

A

THESIS

submitted to the faculty of

THE UNIVERSITY OF MISSOURI-ROLLA

in partial fulfillment of the requirements for the

Degree of

MASTER OF SCIENCE IN CIVIL ENGINEERING

Rolla, Missouri

1969

Approved by

H E Hardaway (advisor) James C. Armstrong

Ronald H. Harrell

ABSTRACT

This study is concerned with the effect of entrained air bubbles on the open-channel hydraulics of water flowing at low velocities. The air bubbles are introduced into the flowing water by injecting diffused compressed air along the channel bottom.

The variations of the velocity profile and velocity distribution energy coefficient of aerated and nonaerated flow are discussed. Empirical equations have been determined for the air concentration and increased depth of flow or "bulking" of the aerated open-channel flow. The investigation revealed a significant increase in the Manning roughness coefficient and the related Darcy friction factor for aerated flow relative to those for nonaerated open-channel flow. Empirical equations are presented which relate the Manning roughness coefficient and Darcy friction factor of aerated flow to the depth, velocity, and Reynolds number of nonaerated open-channel flow.

The results of this investigation are valid only within the range of depths and velocities studied and are further restricted to the geometry and pressure range of the particular air diffuser system utilized in the study.

ACKNOWLEDGMENTS

The writer wishes to express his sincere appreciation to Dr. T. E. Harbaugh for his suggestion of this project and his encouragement throughout this study.

Appreciation is extended to Dr. J. C. Armstrong and Dr. R. H. Howell for their critical review of this thesis and constructive comments.

Special thanks is extended to Mr. H. Hollingsworth for his suggestions and aid during the construction of the experimental apparatus.

Lastly, the writer's wife Helen, deserves special recognition for the many hours she spent at the author's side during the construction and final writing of this project.

TABLE OF CONTENTS

LIST OF ILLUSTRATIONS

Figure Page

LIST OF TABLES

NOMENCLATURE

A = total cross-sectional area, square feet

a = depth of flow, feet

B = coefficient of "bulking" (ratio of depth of aerated flow to that of nonaerated flow), percent

b = height of sluice gate opening, feet

c = air concentration within an elemental area (volume ratio of air to water), percent

c_A = average air concentration within an elemental area for a number of aerated flows, percent

c_a = air concentration at depth (a), percent

c_y = air concentration at depth (y), percent

$\overline{c}$ = mean air concentration of total flow area, percent

C_c = coefficient of contraction

C_d = coefficient of discharge

C_R = ratio of air concentration of "maximum air" aerated flow to that of "minimum air" aerated flow

C_v = coefficient of velocity

CFS = cubic feet per second

d = depth of flow, feet

E = specific energy, feet

f = Darcy friction factor

g = gravitational acceleration, 32.2 feet per second^2

H = total head, feet

h_f = head loss, feet

L = length of channel reach, feet

n = Manning roughness coefficient

P = wetted perimeter, feet

Q = total discharge, cubic feet per second

q = discharge per unit width of channel, square feet per second

R = hydraulic radius, feet

R_e = Reynolds number

s = sine of slope angle

S_f = friction slope, feet per feet

S_o = slope of channel bottom, feet per feet

V = mean velocity of flow, feet per second

v = velocity of flow through an elemental area, feet per second

V_{max} = maximum velocity of flow, feet per second

V_s = velocity of rising air bubbles, feet per second

w = unit weight of water, pounds per cubic feet

x = distance along channel, feet

y = depth of flow, feet

y_{max} = maximum depth of flow, feet

y_m = mean depth of flow, feet

y_1 = depth of flow upstream of sluice gate, feet

z = distance from datum line to channel bottom, feet

α = velocity distribution energy coefficient

ε = coefficient of diffusion

σ = standard error of correlation

υ = kinematic viscosity, centistokes

θ = bottom slope angle, degrees

$^{\circ}F$ = degree Fahrenheit

∂ = partial derivative of

Δ = elemental change in quantity

$\int$ = integral of

Σ = summation of

I. INTRODUCTION

At the present time, considerable emphasis is being given to the purification of our rivers, canals, and lakes by increasing the dissolved oxygen content of the water. Various methods are being considered or are already in use which cause air, in the form of small bubbles, to become entrained in the water for a sufficient time to allow a portion of the oxygen content of the air to be transferred to the water as dissolved oxygen.

Although there has been considerable research concerning the oxygen transfer process associated with the entrained air bubbles in the water or sewage, very little research has been undertaken concerning the effect of the entrained air bubbles on the hydraulic characteristics of the fluid when it is flowing by gravity with a free surface. This type of flow is defined as open-channel flow; this is the usual state of motion of the water or sewage when the previously mentioned aeration processes occur.

It is the purpose of this investigation to study the effect of entrained air bubbles on the open-channel hydraulics of water at low velocities. The air entrainment was accomplished by introducing compressed air, at near minimum pressure, into the flowing water from minute, equally-spaced holes located in the bottom of an open-channel flume. The

discharge of the open-channel flow was controlled by an adjustable sluice gate at the flume outlet which produced varied, subcritical flow with a backwater curve. Uniform flow was not investigated as it was impossible to obtain stable uniform flow at sufficient depths with the available open-channel flume and water supply system.

The objectives of this investigation are fourfold:

1. To compare velocity profiles and velocity distribution energy coefficients of aerated and nonaerated open-channel flow;
2. To study the concentration of air bubbles in the aerated flow;
3. To study the increase in depth, "bulking", of the flowing water due to the presence of the entrained air bubbles; and
4. To determine the effect of the entrained air bubbles on flow retardance by including this effect in the conventional Manning roughness coefficient and the related Darcy friction factor.

II. LITERATURE REVIEW

Aerated open-channel flow, as described in this investigation, is a mixture of water and entrained air bubbles flowing in a channel, having a free surface subject to atmospheric pressure (i.e. open channel).

Aerated flow may occur naturally in open channels of steep slope having high-velocity flow and an accompanying high degree of turbulence. Lane[1]* concluded that the minimum degree of turbulence necessary for air entrainment to occur naturally is that turbulence existing when the turbulent boundary layer intersects the free surface. Here, agglomerations of water particles which possess a velocity component normal to the surface escape into the overlying atmosphere. This phenomenon occurs when the momentum of a particular agglomeration of particles is large enough to overcome the restraining force of surface tension. When the particles return again to the body of water due to gravitational force, they entrap air which is carried in the form of bubbles of varying size from the surface to deeper depths by the action of turbulent diffusion. This diffusion action, however, is opposed by the bouyant force on each bubble causing the concentration of air at any depth within the flow to vary from a maximum at the free surface to a minimum

---

*Raised numbers in parentheses refer to references listed in Bibliography.

at the channel bottom. This type of aerated open-channel flow is defined as self-aerated flow.

In 1955, Straub and Anderson[2] concluded that the mean air concentration ($\overline{c}$) of self-aerated flow in smooth channels is a function of $(s/q)^{2/3}$ where s is the sine function of the slope angle and q is the discharge per unit width of channel. Later in 1958, Straub and Anderson[3] reported that $\overline{c}$ for self-aerated flow in rough channels was a function of $(s/q)^{1/5}$. They also concluded the following:

1. Self-aerated open-channel flow consists of two distinct phases: an upper region consisting of a bubble layer with water droplets intermixed which moves at a lower velocity than and independent from the stream proper, and a lower region in which discrete air bubbles are suspended in a turbulent stream and are distributed by the mechanism of turbulence;
2. The bulking of the aerated flow increases rapidly with mean air concentration;
3. The mean velocity of air-entrained flow is greater than that of a corresponding nonaerated flow by an amount that increases with air concentration and a corresponding decrease in the mean depth; and

4. Self-aerated flow may be described by a formula of the Chezy type involving approximately the same roughness coefficient as applies for nonaerated flow if a depth which excludes the bubble layer is used.

Aerated flow may also occur in open channels of mild slope having low velocities of flow. However, in this type of aerated flow, the air must be entrained in the flowing water by a means other than the mechanism of a high degree of surface turbulence produced by high velocity flow, as in self-aerated flow. In low-velocity aerated flow the air enters the flowing water as the result of energy being applied. This energy originates externally from the flowing water itself. Examples of this type of aeration are:

1. A high-velocity water jet discharging into open-channel flow can produce sufficient turbulence at the free surface to cause air to become entrained by the same mechanism (surface turbulence) as in self-aerated flow; the jet also contributes air directly to the water as the result of air entrained at the boundaries of the jet or within the volume of the jet itself;
2. Mechanical agitators can produce sufficient turbulence in open-channel flow to cause air to become entrained at the free surface, as in self-aerated flow; and

3. Diffused compressed air can be injected into open-channel flow.

Einstein and Sibul[4], in 1954, investigated low-velocity aerated flow where the air entrainment was produced by an isotropic turbulence created by water jets discharging into the open-channel flow. The turbulence was evenly distributed over the water depth and slowly diminished to an insignificant intensity at some point downstream of where the jets discharged. They derived the following relationship for the air concentration at any depth of flow:

$$\ln (c_y/c_a) = -[V_s (y-a)] / \varepsilon$$

where c_y and c_a are the air concentrations at depths y and a respectively, V_s is the rising velocity of the entrained air bubbles, and ε is a diffusion coefficient that must be found experimentally for a given turbulent condition. They also determined that the percentage of water in the aerated flow was a function of the depth or velocity of the aerated and corresponding nonaerated flow.

In 1934, Townsend[5] reported on a small number of observations concerning the retarding effect of entrained air bubbles on the flow of a mixture of sewage and activated sludge through a conventional activated sludge sewage treatment unit. Compressed air was introduced into the sewage through porous plates located along the bottom of the activated sludge basin forming a ridge-and-furrow type aeration

pattern. Townsend chose to approach the problem of determining the degree of flow retardance caused by the diffused compressed air by assuming the following:

1. Although the total suspended matters in the mixture of sewage and activated sludge was about 3000 ppm, the hydraulic properties of the mixture were considered the same as for water alone; and
2. The density and hydraulic properties of water containing entrained air bubbles were considered the same as for water alone.

As a result of his observations, Townsend concluded the following:

1. Resistance to flow increases because of entrained air bubbles and this resistance may be expressed in terms of an increase in the Manning roughness coefficient (n); and
2. The flow retardance due to the entrained air increases as the flow velocity decreases.

Townsend attributed the increase in Manning's n to the added wetted perimeter of the air bubbles and thus a corresponding decrease in the hydraulic radius. Also, he stated that the increase in flow retardance corresponding to a decrease in flow velocity was due to greater coalescence (the combining of two or more individual bubbles into a single bubble) at higher velocities which resulted in a decrease in the total wetted perimeter of the entrained air bubbles.

Thackwell[6] in a discussion of the Townsend report added the following experimental observations of the mechanics of bubble formation in water or sewage:

1. The rise of an air bubble introduced as compressed air from a diffuser into water or sewage consists of two separate phases, a) the jet action phase and b) the individual bubble floatation phase;
2. The height of the jet action varies directly with the volume of air and the type of air diffuser;
3. The floatation phase occurs when the jet of air accelerates upward and encounters resistance from the water, whereupon it breaks into individual bubbles of various sizes which change from circles to deformed oblate spheroids as they float upward at uniform velocity;
4. The specific gravity of a mixture of entrained air and water may be taken as that of water alone provided no allowance is made for the increase in water depth due to water being displaced upwards by the volume occuppied by the entrained bubbles;
5. The size and velocity of a bubble remains practically the same throughout its travel range; and
6. Coalescence is the cause of increased bubble size, but this increase in size does not produce increased velocities.

The published literature concerning aerated open-channel flow is not plentiful. The aforementioned being the total available except for that pertaining to the subject of self-aerated flow which thus far has received the principal attention of investigators.

The information on self-aerated flow by Stroud and Anderson[2,3] and that on aeration due to jet action by Einstein and Sibul[4] provide general background information concerning aerated flow. The works of Townsend[5] and Thackwell[6] represent the sum total of available published information concerning the type of aerated open-channel flow of this investigation.

III. THEORY

In this investigation of low-velocity, aerated open-channel flow, the following basic assumptions were made:

1. The hydraulic principles applying to nonaerated open-channel flow were also applicable to aerated flow. Thus the aerated flow could be described by the same hydraulic properties (velocity distribution, velocity distribution coefficient, energy loss coefficients, etc.) used in describing nonaerated open-channel flow;
2. The aerated flow was considered to have the same physical properties, e.g., density, viscosity, etc., as nonaerated flow, i.e., in analyzing the aerated flow, an elemental volume was assumed to contain only water and no air bubbles; and
3. The air injected into the flowing water was considered to affect only the kinematic properties of the flowing water, i.e., the injected air acted upon an elemental volume of water in a manner similar to that which would occur if the injected media were water rather than air.

The aerated flow of this investigation was studied by using basic hydraulic principles normally associated with nonaerated flow. These principles will now be developed in detail.

A. Flow Measurement

A sluice gate may be used to measure the discharge in an open-channel. An equation for the discharge may be derived[7,8,9,10] from the energy equation written between section 1 located upstream of the sluice gate and section 2 located downstream of the gate at the vena contracta of the free (unsubmerged) discharge. The energy equation, when the datum plane is taken as the channel bottom and the energy coefficients α_1 and α_2 are both assumed equal to 1.0, may be written as:

$$\frac{V_1^2}{2g} + y_1 = \frac{V_2^2}{2g} + y_2 + h_f \qquad (1)$$

where: V = mean velocity, ft/sec;

y = depth of flow, ft;

g = gravitational acceleration, 32.2 ft/sec^2; and

h_f = head loss between sections 1 and 2, ft.

Applying the principle of continuity of flow gives the relationship:

$$q = V_1 y_1 = C_v V_2 C_c b \qquad (2)$$

where: q = discharge per unit width of channel, ft^2/sec;

C_v = velocity coefficient to include effect of head loss;

C_c = coefficient of contraction of the free discharge at the vena contracta; and

b = height of gate opening, ft.

Also, if the depth y_2 is small in relation to y_1, then it can be shown that the head loss between sections 1 and 2 may be expressed as:

$$h_f = \left(\frac{1}{C_v^2} - 1\right)\frac{V_2^2}{2g} \tag{3}$$

Upon substituting Equation (3) and Equation (2) into Equation (1) and replacing the velocities by the ratios of unit discharge to depth, Equation (1) becomes:

$$\frac{q^2}{2gy_1^2} + y_1 = \frac{q^2}{2gC_v^2C_c^2b^2} + C_cb \tag{4}$$

Solving for q results in the relationship:

$$q = \frac{C_vC_cb\sqrt{2g\,(y_1 - C_cb)}}{\sqrt{1 - C_v^2C_c^2b^2/y_1^2}} \tag{5}$$

Since the values of C_v and C_c are difficult to obtain experimentally, Equation (5) is usually expressed as:

$$q = C_db\sqrt{2gy_1} \tag{6}$$

where:
$$C_d = \frac{C_vC_c\sqrt{1 - C_cb/y_1}}{\sqrt{1 - C_v^2C_c^2b^2/y_1^2}}$$

When the channel is rectangular in shape with a width of 2.0 feet, the total discharge (Q) may be expressed as:

$$Q = 2bC_d\sqrt{2gy_1} \tag{7}$$

Thus, the channel discharge (Q) may be easily calculated from Equation (7) by knowing the upstream depth (y_1), the gate height (b), and the value of the coefficient of discharge (C_d). Since C_d depends on y_1 and b, a relatively simple calibration of the sluice gate is required. The calibration essentially involves the measurement of Q for various combinations of y_1 and b. Rearranging Equation (7) to the form:

$$C_d = \frac{Q}{2b\sqrt{2gy_1}} \tag{8}$$

allows the calculation of C_d for each combination of y_1 and b. Plotting C_d against the ratio y_1/b, provides a simple method of determining the particular C_d to use in Equation (7), along with the corresponding y_1 and b values, for computing the channel discharge (Q).

B. Determination of Velocity Distribution Energy Coefficient

The kinetic energy per unit of time of a weight of water (w) passing through an area of elementary size (ΔA) with a velocity (v) is equal to the product of the weight ($wv\Delta A$) and the velocity head ($v^2/2g$). The total kinetic energy for the sum of the elementary areas (ΔA) which make up the total area (A) of flowing water is equal to the quantity $(\Sigma wv^3\Delta A/2g)$[7,8].

Also, taking the total area (A), the mean velocity (V) of the total area, and a corrected velocity head for the

total area ($\alpha V^2/2g$), where α is a correction coefficient equal to or greater than unity, results in the total kinetic energy being equal to the quantity ($\alpha w V^3 A/2g$). Equating this quantity with the quantity ($\Sigma w v^3 \Delta A/2g$) results in Equation (9):

$$\alpha = \frac{\int v^3 \partial A}{V^3 A} \simeq \frac{\Sigma v^3 \Delta A}{V^3 A} \tag{9}$$

where:

$$V \simeq \frac{\Sigma v^3 \Delta A}{A} \tag{10}$$

Equation (9) may be solved graphically as follows:

Equal velocity contours are drawn through a plot of the point velocity measurements taken over a grid pattern of the flow cross-section. A planimeter is used to determine the area within each contour interval. The summation of the products of the cube of the mean velocity within each contour interval and the area of that contour interval, when divided by the product of the cube of the velocity (V) of the total flow and the total area (A), gives the value of the velocity distribution energy coefficient (α).

C. Determination of Mean Air Concentration

If c is the ratio percent of air to water in an area of elemental size (ΔA) within the total flow area (A), then the mean air concentration ($\overline{c}$) of the total area may be determined by Equation (11):

$$\overline{c} = \frac{\int c\,\partial A}{A} \simeq \frac{\Sigma c \Delta A}{A} \qquad (11)$$

Equation (11) may be solved utilizing a graphical method similar to that previously described for the solution of Equation (9).

D. Gradually Varied Flow

When a sluice gate is installed in an open channel having steady flow, the flow will back-up behind the gate such that the depth of flow gradually decreases along the reach of channel in an upstream direction from the gate. The resulting flow is a type of gradually varied flow[7,8,9,11]. The uniform flow equations of Manning and Chezy are invalid for this type of flow.

Referring to Figure 1, the total head at the upstream section 1, above the datum plane coinciding with the channel bottom, is:

$$H = z + d \cos \theta + \alpha V^2/2g \qquad (12)$$

where: H = total head, ft;

z = distance from datum line to channel bottom

d = depth of flow, ft;

θ = bottom-slope angle;

α = velocity distribution energy coefficient; and

V = mean velocity, ft/sec.

It is apparent that, with a constant flow rate (Q), the depth (d) and the mean velocity (V) are a function of the

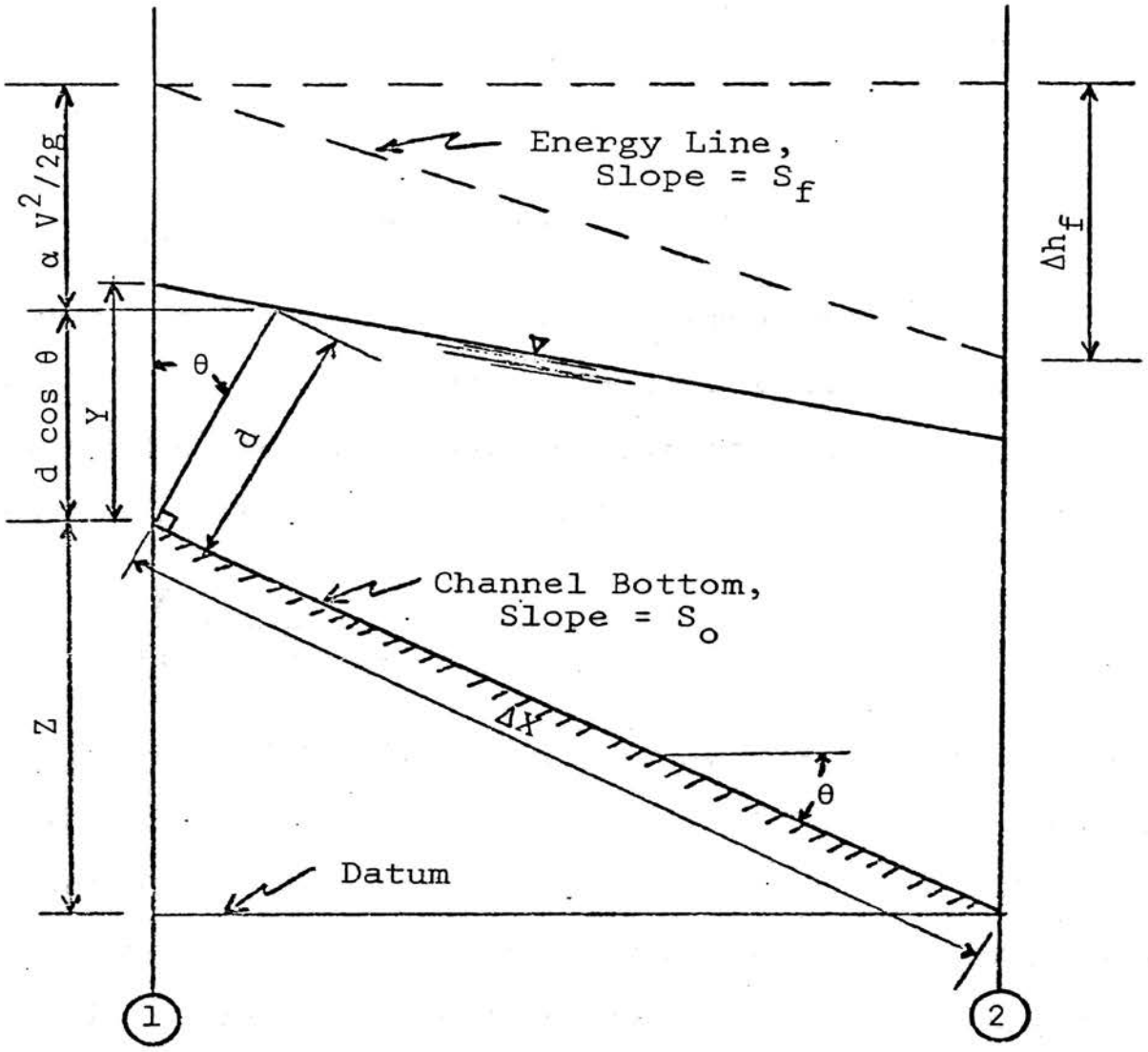

FIGURE 1. ELEMENTAL REACH OF OPEN CHANNEL WITH GRADUALLY VARIED FLOW FOR DERIVATION OF THE DIFFERENTIAL EQUATION OF GRADUALLY VARIED FLOW

distance (x) measured along the channel bottom. The values of α and θ are assumed constant throughout the channel reach under consideration and θ is considered small. Thus, y = d, and Equation (12) may be differentiated with respect to x to obtain:

$$\frac{\partial H}{\partial x} = \frac{\partial z}{\partial x} + \frac{\partial y}{\partial x} + \frac{\partial(\alpha V^2/2g)}{\partial x} \qquad (13)$$

Since the friction slope (S_f) is equal to $-\partial H/\partial x$, and the slope of the channel bottom (S_o) is equal to sin θ or $-\partial z/\partial x$, Equation (13) may be rewritten as the differential equation of gradually varied flow:

$$\frac{\partial y}{\partial x} = \frac{S_o - S_f}{1 + \partial(\alpha V^2/2g)/\partial y} \qquad (14)$$

Equation (14) may be solved by the direct step method for the flow profile. The distance (x) is thus determined for which a given change in the depth (y). In this method the channel is divided into short reaches of length (Δx), as shown in Figure 2. Assuming the uniform flow equations of Manning or Chezy are valid, the computation is performed step by step along the channel from a point of known depth to any desired upstream point.

The value of Δx corresponding to a relatively small change in y is computed by equating the heads at the two end-sections 1 and 2, of Figure 2. Thus,

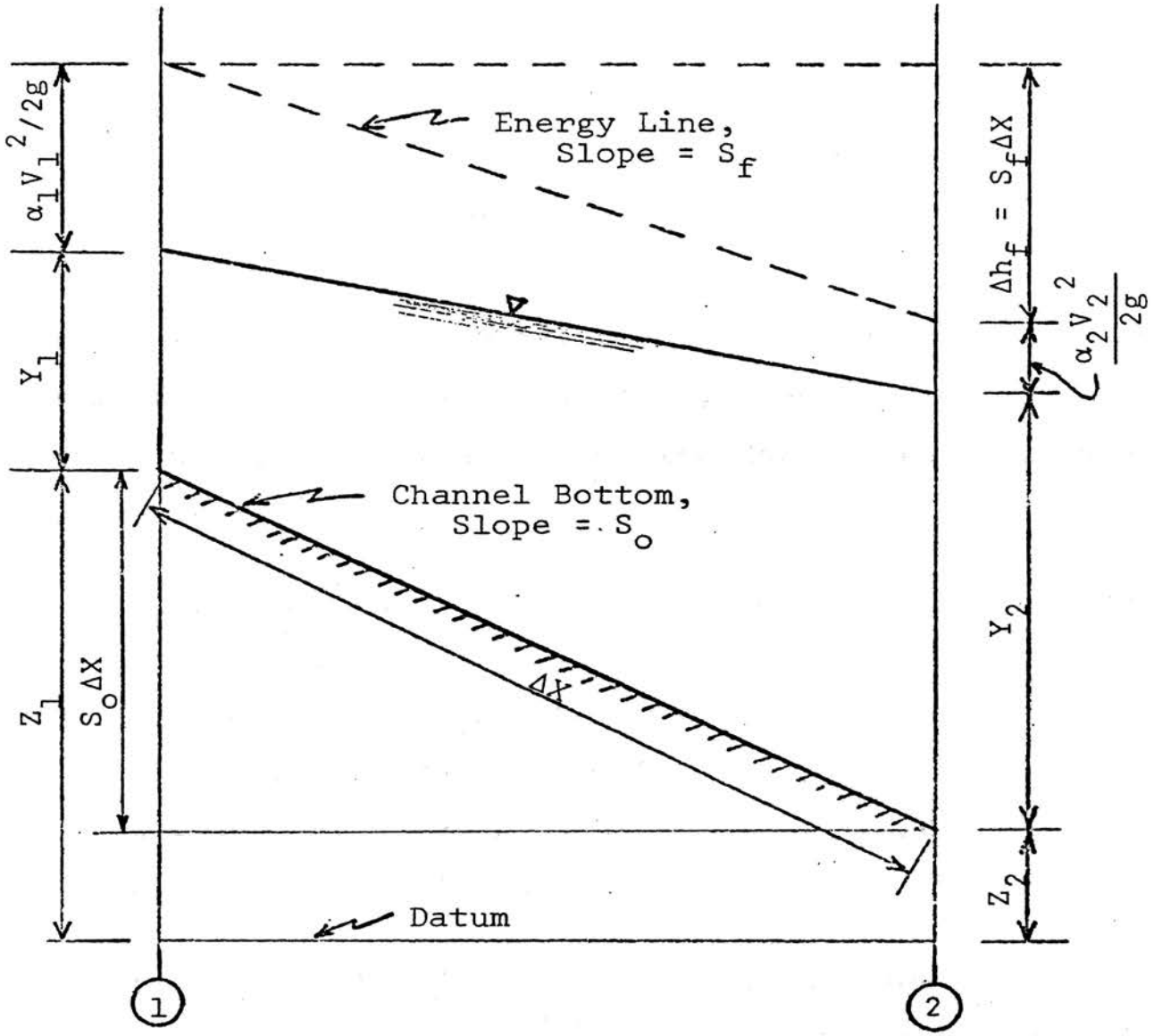

FIGURE 2. ELEMENTAL REACH OF OPEN CHANNEL WITH GRADUALLY VARIED FLOW FOR DERIVATION OF THE DIRECT STEP METHOD SOLUTION OF THE DIFFERENTIAL EQUATION OF GRADUALLY VARIED FLOW

$$S_o \Delta x + \frac{y_1}{2g} + \alpha_1 V_1^2 = y^2 + \frac{\alpha_2 V_2^2}{2g} + S_f \Delta x \qquad (15)$$

Solving for Δx yields:

$$\Delta x = \frac{E_2 - E_1}{S_o - S_f} = \frac{\Delta E}{S_o - S_f} \qquad (16)$$

where E is the specific energy at a section and is equal to the sum of the depth (y) and velocity head ($\alpha V^2/2g$) at that section. S_f can be computed from the Manning equation written in the form:

$$S_f = \frac{n^2 V^2}{2.22\ R^{4/3}} \qquad (17)$$

where: n = Manning's roughness coefficient;

R = hydraulic radius = A/P, ft;

A = area of flow cross section, ft^2; and

P = wetted perimeter, ft.

E. Determination of n for Gradually Varied Flow

The direct step method[7,8] is normally employed to determine the distance along the channel reach at which a specified depth of flow occurs. In this situation the variables which are known (measured or assumed values) are:

1. The depth of flow (y_1) at an initial point along the channel reach, usually at the point of flow control (in this case the sluice gate);
2. The depth of flow (y_2) which is specified;

3. The steady discharge (Q);
4. The channel geometry, which must be prismatic when using the direct step method; and
5. The Manning roughness coefficient (n).

The value of the distance (L) along the channel reach from y_1 to y_2 is then determined by the summation of all the Δx values as computed in the direct step method utilizing Equation (16).

The direct step method may also be employed in reverse to determine one of the above known values if the distance (L) is known. Thus, the Manning n may be determined if L, y_2, Q, and the channel geometry are known. Here a value of n is assumed, and the distance (L) computed from the direct step method is compared with the actual distance (L) between the points at which (y_1) and (y_2) occur. If the computed value does not agree with the actual value, another value of n is selected and the procedure is repeated until the two values of L are the same. The n value at which the two distances agree is the desired value of n for this particular flow condition.

Included in the Appendix is a Fortran IV digital computer program for the iterative solution of n utilizing the direct step method of solving the differential equation of gradually varied flow.

F. The Manning n and Darcy Friction Factor (f)

The Manning n as applied to gradually varied flow may be expressed by rewriting Equation (17) as:

$$n = \frac{1.486\ R^{2/3}\ S_f^{1/2}}{V} \tag{18}$$

where the friction slope (S_f) is an energy gradient defined as the energy loss (h_f) divided by the distance (L) along the channel and over which the energy loss occurred. The energy loss in gradually varied open channel flow is:

$$h_f = S_o L + (y_1 - y_2) + (V_1^2 - V_2^2)/2g \tag{19}$$

The Darcy-Weisbach formula[7] for open-channel flow is:

$$h_f = f\ \frac{L}{4R}\ \frac{V^2}{2g} \tag{20}$$

Replacing h_f/L by S_f and rearranging yields:

$$S_f = \frac{fV^2}{8gR} \tag{21}$$

Substituting this expression into Equation (18) for S_f and solving for f yields:

$$f = \frac{116\ n^2}{R^{1/3}} \tag{22}$$

Equation (22) provides a means of relating the Manning n to parameters conventionally used with the Darcy friction factor (f) such as the Reynolds number (Re). The Reynolds number for open-channel flow is:

$$Re = \frac{VR}{\nu} \tag{23}$$

where ν is the kinematic viscosity of the fluid.

G. Flow Retardance

The retardance of flow in open channels is usually evaluated in terms of the Manning roughness coefficient (n) while flow retardance in pipes is associated with the Darcy friction factor (f). In both cases, the flow retardance factor accounts for the energy losses that occur as a result of the frictional resistance encountered at the channel boundary. However, it is well known that energy losses other than those due to boundary frictional resistance also occur in open-channel flow, i.e., losses due to secondary flow, eddies, etc. When an n or f value is determined for a straight, uniform length of channel or pipe, these other energy losses, if present, are combined with the boundary frictional resistance. Therefore, in this investigation the flow retardance due to the injected air will likewise be evaluated in terms of the Manning roughness coefficient (n) or the Darcy friction factor (f). However, if one objects to this liberty, the n and f values so determined may be thought of as an apparent n and f.

IV. EXPERIMENTAL APPARATUS

The plexiglass open-channel flume, shown in Figure 3, was the principal apparatus employed in this investigation. The flume measured 36 feet in length, and 2 feet in both height and width. A plexiglass false-bottom, as shown in Figure 4, consisting of eighteen separate compartments each 2 feet in both length and width and 2 1/2 inches in height, was constructed and placed along the bottom of the flume for the purpose of diffusing compressed air into water flowing in the flume.

Compressed air from a centrifugal blower, rated at 300 cubic feet per minute at 15 inches of water pressure, discharged into a 3 inch diameter plastic header pipe, as shown in Figure 5. Fourteen 1 1/2 inch diameter valved takeoffs, as shown in Figure 6, routed the air to the centermost fourteen compartments of the plexiglass false-bottom. The air then passed into the flume interior through minute holes (0.040 inches in diameter) drilled through the 3/8 inch thick plexiglass false-bottom, as shown in Figure 7. The holes were equally spaced on 1 inch centers, commencing 1/2 inch from the sides of the flume. U-tube water manometers, as shown in Figure 6, were provided at each of the fourteen air distribution compartments to monitor the air pressure.

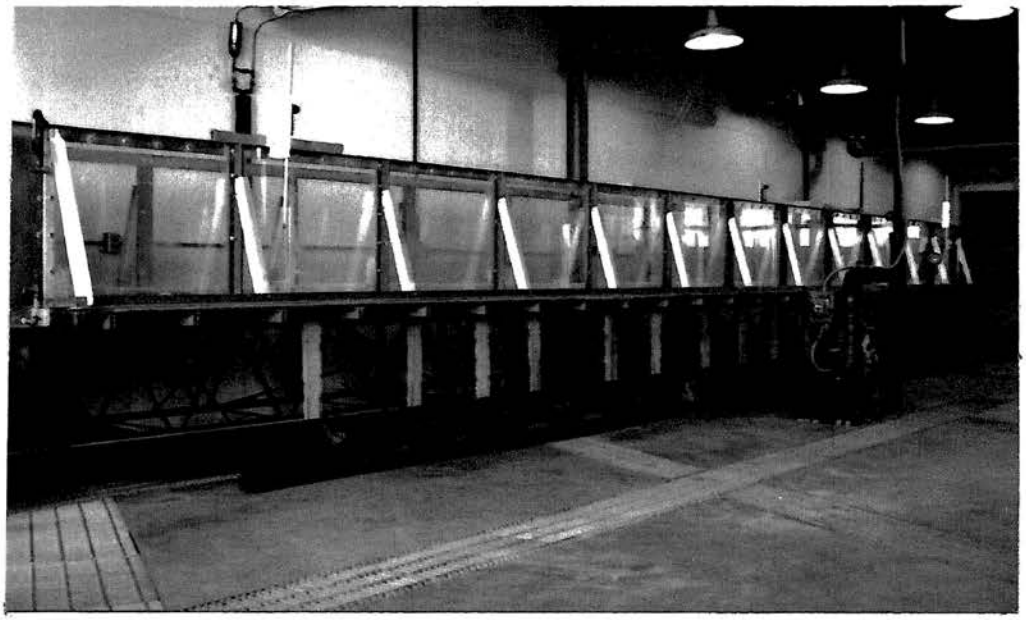

FIGURE 3. GENERAL VIEW OF EXPERIMENTAL APPARATUS

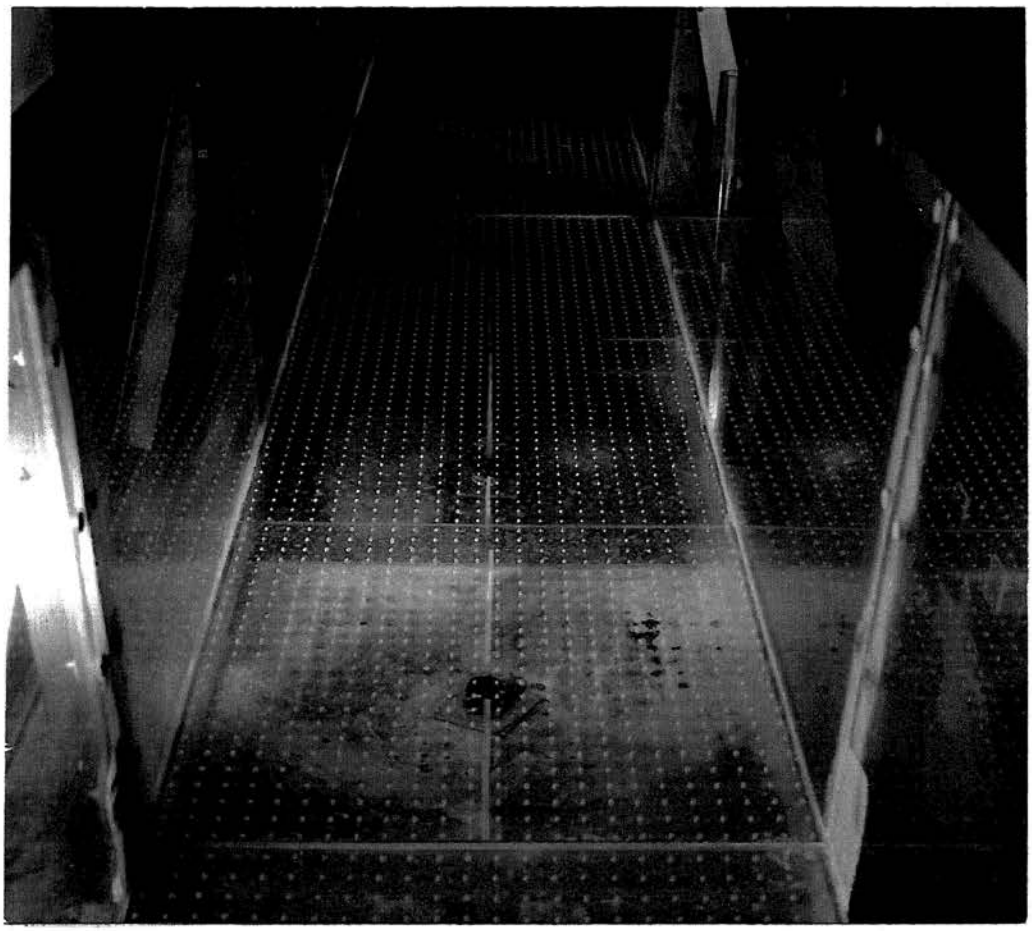

FIGURE 4. PLEXIGLASS FALSE-BOTTOM OF OPEN-CHANNEL FLUME

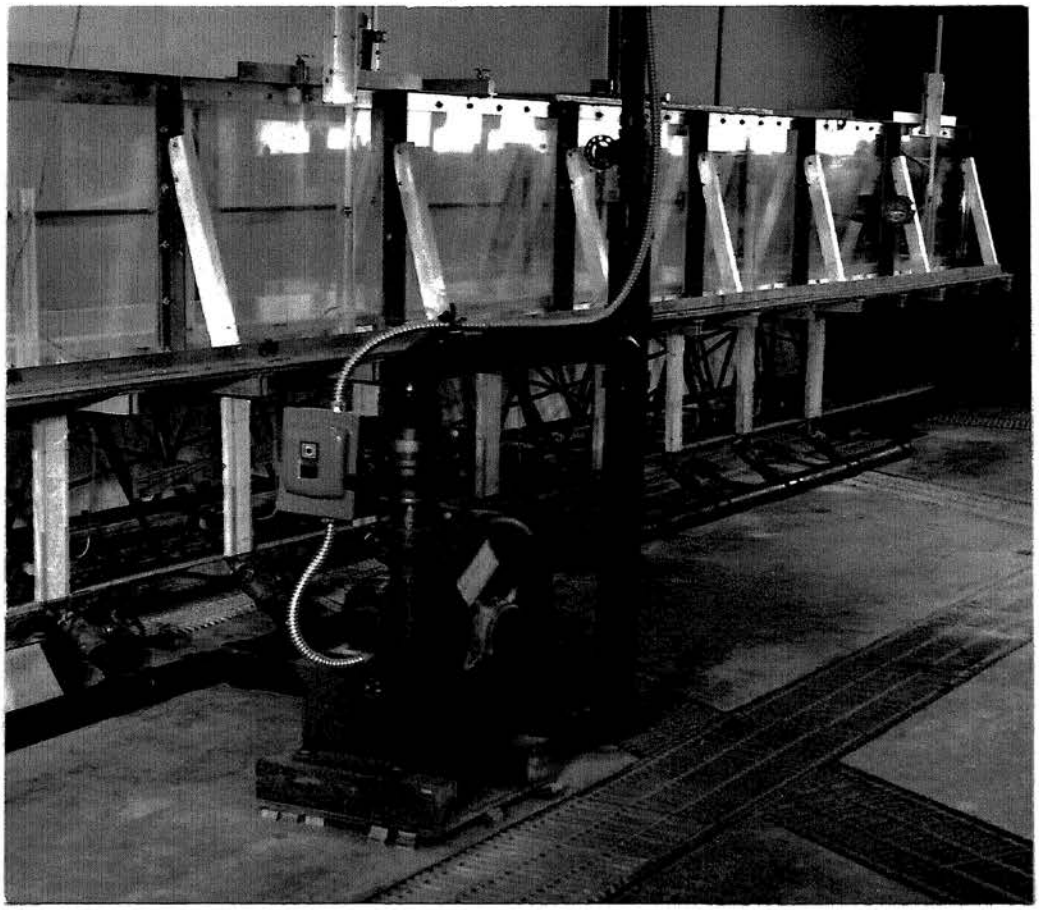

FIGURE 5. COMPRESSED AIR SYSTEM

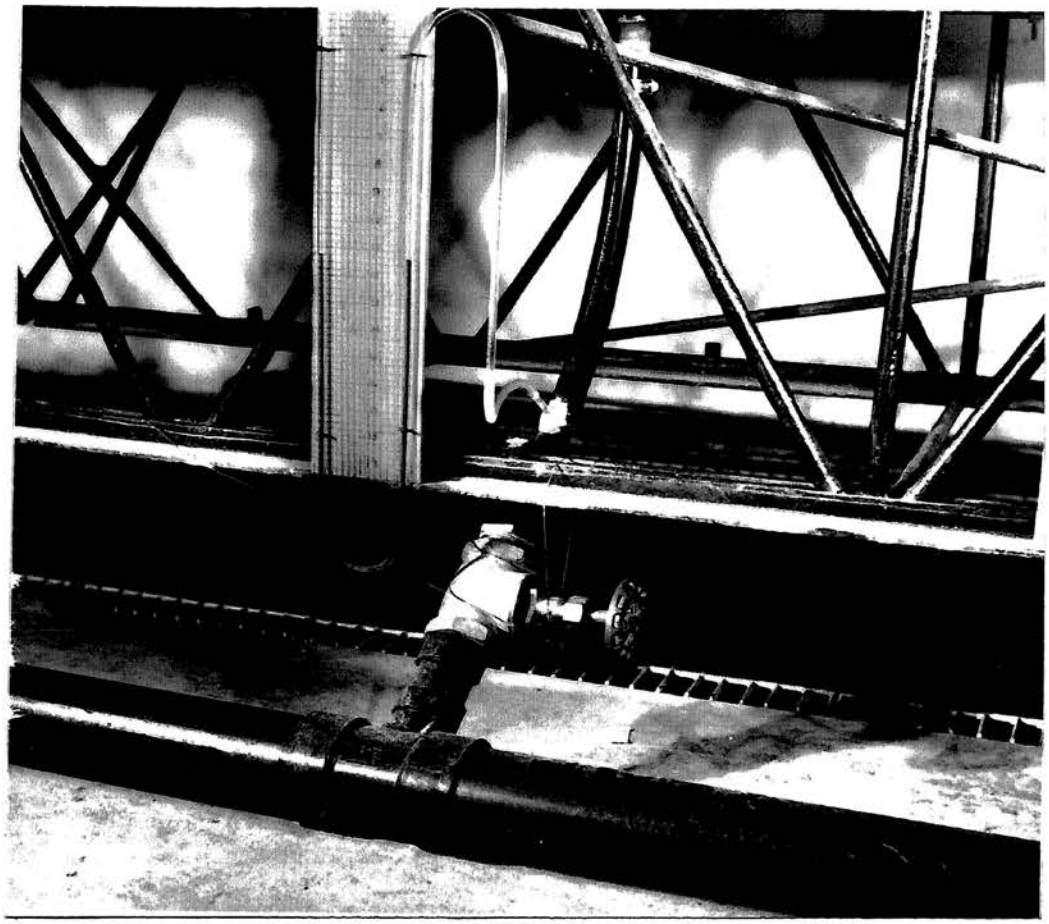

FIGURE 6. COMPRESSED AIR INLETS TO FALSE-BOTTOM OF FLUME AND U-TUBE MANOMETERS

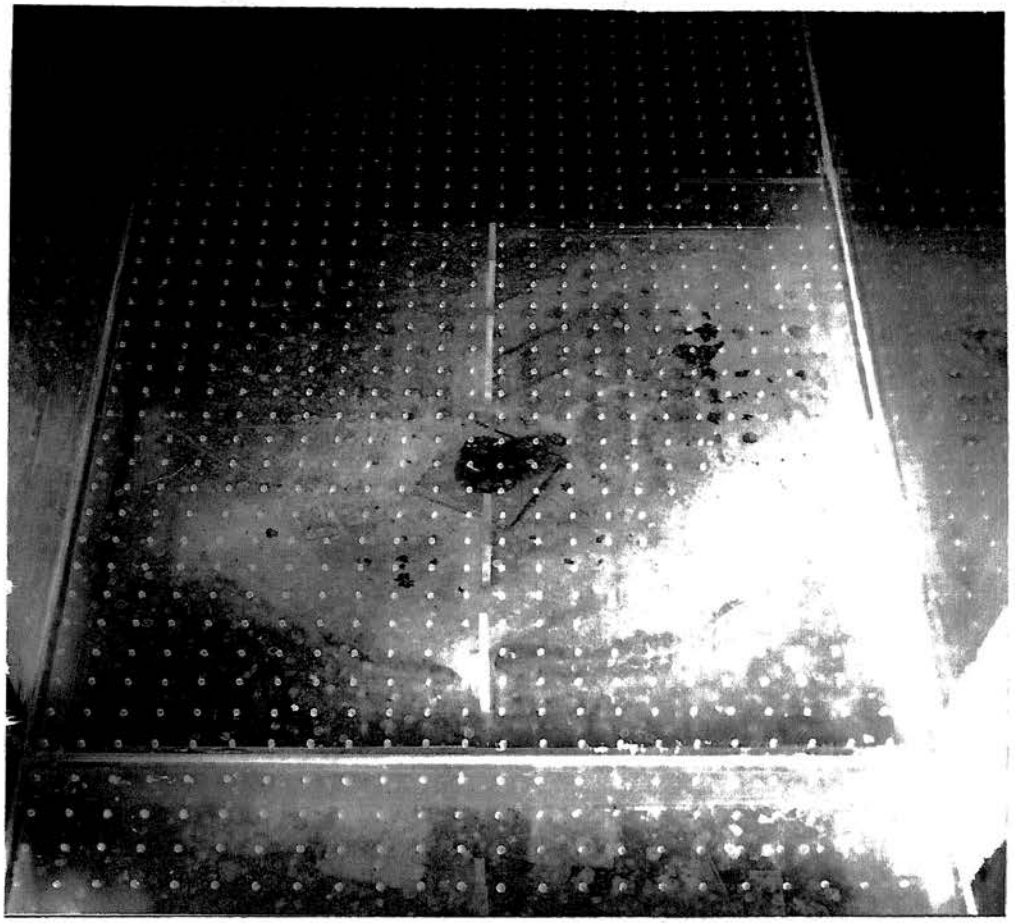

FIGURE 7. AIR DISTRIBUTION HOLES IN PLEXIGLASS FALSE-BOTTOM

Depth of flow measurements were taken in stilling wells constructed of 1 1/2 inch diameter clear plastic pipe, as shown in Figure 8, located at intervals along the length of the flume. The wells were connected to the flume interior with 1/4 inch inside diameter plastic tubes. The wells proved very effective in damping-out minor fluctuations in the depth of the flowing water. Depths were measured using point gauges graduated in one-thousandths of a foot.

The water supply was obtained from a recirculating system having a centrifugal pump capable of delivering approximately 2.5 cubic feet per second. The flow of water to the flume was regulated by a 6 inch gate valve connected to a 12 inch recirculating header pipe.

The scale of turbulence at the inlet of the flume was significantly reduced by installing a flow-through horizontal baffle, as shown in Figure 9, consisting of two perforated aluminum plates, having equally-spaced 1 inch diameter holes, with a sheet of stainless steel, fine-meshed screenwire sandwiched between the two plates.

Varied flow was controlled in the flume by a sharp-edged sluice gate located at the outlet end of the flume, as shown in Figure 8. The gate was 2 feet in width and 6 inches in height, and was mounted to the sides of the flume with adjustable clamps.

FIGURE 8. STILLING WELL AND SLUICE GATE

FIGURE 9. FLUME INLET WITH HORIZONTAL FLOW-THROUGH BAFFLE

Air concentrations were taken with a resistance probe[12], as shown in Figure 10, powered by an audio frequency oscillator (24.5 volt at 600 ohm, 20 to 40,000 cycles per second) with the measurements observed on a standard voltmeter. The resistance probe consisted of two stainless steel electrodes (3/4 inch long x 3/8 inch high x 1/16 inch thick) spaced 3/8 inch apart and mounted to the end of a 1 inch diameter x 12 inches long steel pipe with a plexiglass insulation mounting adaptor. The edges and back sides of the electrodes were covered with an insulation coating. The resistance probe was connected to the audio oscillator, variable resistor, and voltmeter with shielded cable, as shown in Figure 11. The resistance probe was mounted on an x-y traverse to facilitate its accurate positioning at all points within the flume.

Velocity measurements were taken with a calibrated Price pygmy current meter. Auxillary equipment included a stopwatch, weighing tank mounted on a scale, thermometer, dumpy level, cathometer, and a planimeter.

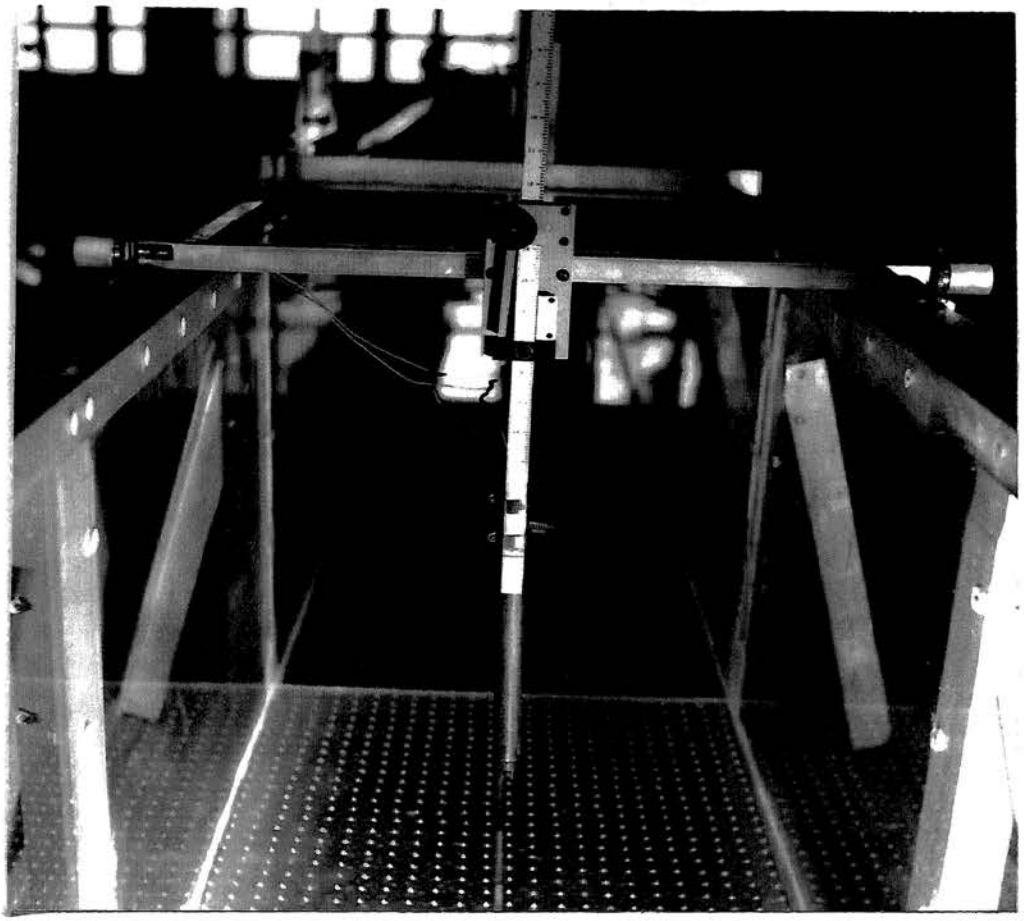

FIGURE 10. AIR CONCENTRATION PROBE MOUNTED ON X-Y TRAVERSE

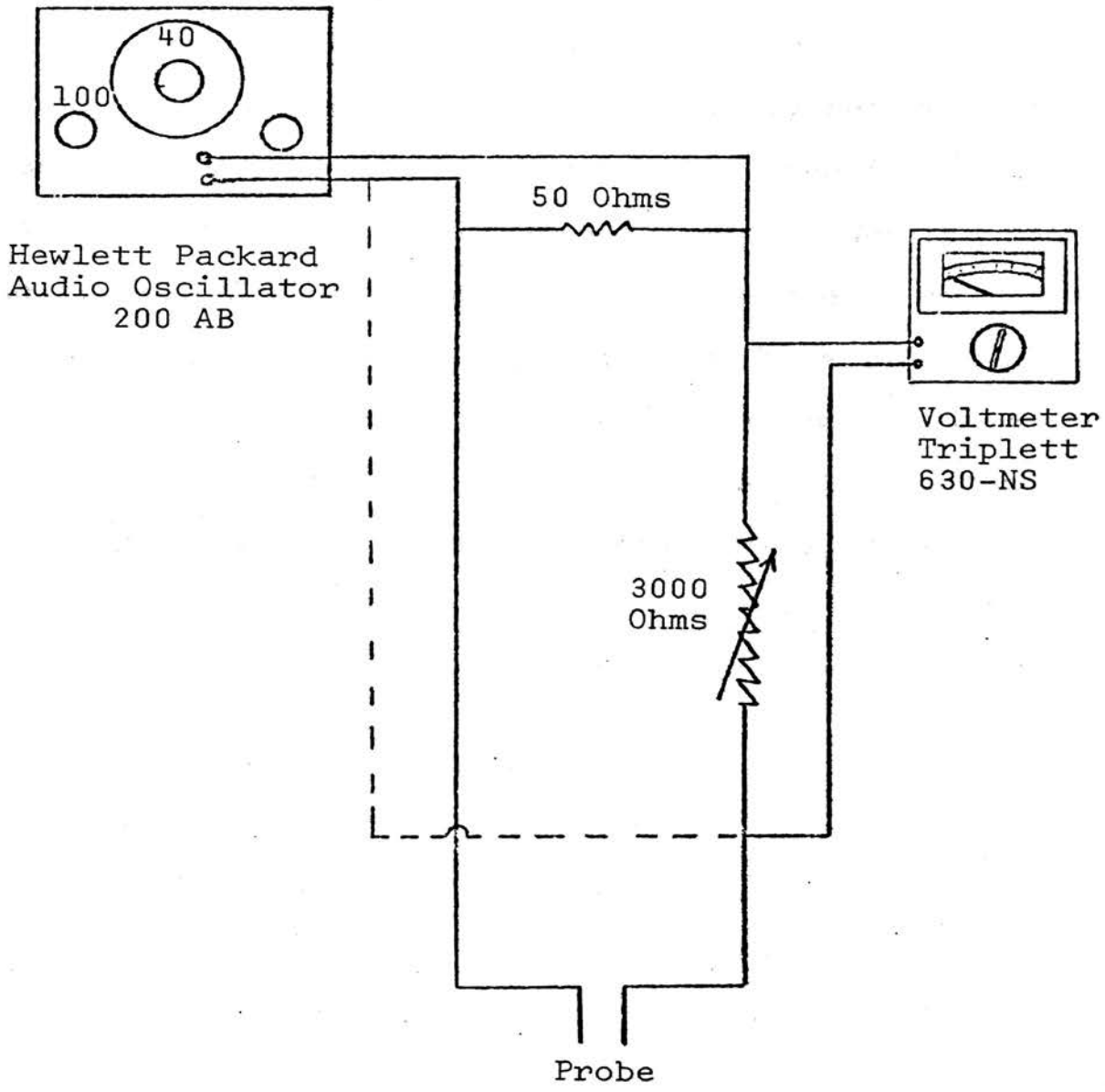

FIGURE 11. SCHEMATIC OF ELECTRICAL CIRCUIT OF AIR CONCENTRATION PROBE

V. EXPERIMENTAL PROCEDURES

A. Referencing for Depth Measurements

In order to obtain the desired precision in the data analysis, it was essential to accurately reference the channel bottom to the point gauges mounted in the stilling wells. A dumpy level was used to set the desired slope of the flume. The reference points along the flume bottom included those directly opposite the three stilling wells. A cathometer was used to initialize the point gauges by aligning the gauge tips with the flume false-bottom. The stilling wells were located at stations 0.00, 12.10, and 30.33, measured in feet, with station 0.00 located 1.75 feet upstream from the sluice gate at the flume outlet.

B. Sluice Gate Calibration

The sluice gate was calibrated by 45 test runs. Three gate heights were used so as to provide a range of discharges varying from 0.3 to 1.3 CFS. The depth y_1 was measured 1.75 feet upstream from the gate. A weighing tank mounted on scales, which were preset to weigh 1400 pounds of water, was moved to intercept the gate discharge; a stopwatch was simultaneously activated to record the elapsed time until the scale arm started moving upward. To improve the accuracy of this calibration, the added weight, due to the force of the water entering the tank, was determined by an iterative procedure, and then subtracted from the weight of water

intercepted during the recorded time interval. The discharge coefficient (C_d) was then plotted against the ratio (y_1/b). All measurements and calculations were made to three significant figures.

C. Operation

Only thirteen of fourteen aeration compartments were used throughout the investigation, since entrained air bubbles emitted from the air diffuser compartment immediately upstream from the stilling well at station 0.00 caused excessive fluctuations in the water level in this stilling well. This condition was minimized by shutting off the first aeration compartment; thus, this investigation was only concerned with 26 feet of aerated open-channel flow.

D. Flow Velocity Measurements

Velocities were determined with a Price pygmy current meter for representative nonaerated and aerated flows at selected grid points across the flow-section at station 12.10. The mean velocity (V) and velocity distribution energy coefficient (α) were then determined by a graphical method.

E. Air Concentration Measurements

Air concentrations (c) of various aerated flows were determined, with the resistance probe and voltmeter at selected grid points across the flow-section at stations 8.25 and 26.30. The mean air concentration at each station was determined by a graphical method similar to that used in

determining the mean velocity. The average of the means of the two stations was recorded as the mean air concentration ($\overline{c}$) of that particular rate of aerated flow.

F. Bulking Measurements

Depth measurements were taken, at station 12.10, both in the stilling well and in the flume itself for the maximum air and minimum air aerated flows at the same discharges as flow retardance measurements were taken. The depth, measured inside the flume, corresponded to the average maximum height of the bubble layer which floated on top of the air-water mixture. The depth of flow as measured in the stilling well was essentially the depth of a corresponding nonaerated flow.

G. Flow Retardance Measurements

Depths were measured in the stilling wells at stations 0.00 and 30.33 for a range of discharges varying from 0.30 to 1.30 CFS for the following types of flow:

1. Nonaerated flow.
2. Aerated flow.
    a. "Maximum Air": The 1 1/2 inch globe valves regulating the flow of air to the air diffusion compartments were in a wide-open position. The air pressure within the diffusion compartments was greater than the static pressure head due to the depth of flow in the channel above; the excess pressure ranged from 1.8 to 2.4 inches

of water with an average of 2.20 inches of water. This condition of aerated flow will hereafter be referred to as maximum air.

b. "Minimum Air": The previously mentioned valves were in a partially closed position such that just enough air entered the diffusion compartments to cause an even distribution of air into the flowing water, i.e., air was flowing through all of the minute holes in the channel bottom. The excess air pressure within the diffusion compartments ranged from 1.2 to 1.3 inches of water with an average of 1.25 inches of water. This condition of aerated flow will hereafter be referred to as minimum air.

Station 0.00 was located 4.08 feet downstream of the last aeration point and station 30.33 was located 0.20 feet upstream from the first point of aeration.

H. Variation of Slope

The sluice gate calibration, flow velocity, air concentration, bulking, flow retardance measurements were taken with the flume set at the steep slope of 0.004975 and then repeated again with the flume set at the mild slope of 0.001000.

VI. ANALYSIS OF DATA

A. Flow Measurement

A least squares correlation[13] of the coefficient of discharge (C_d) of the sluice gate with the dimensionless ratio (y_1/b) of the upstream depth of flow (y_1) and the height of gate opening (b), is shown in Figure 12. The correlation equation

$$C_d = 0.482(y_1/b)^{0.090} \tag{24}$$

was the result of experimental data from 45 sluice gate calibration tests. The standard error (σ) of the correlation was 0.0064 and the deviation was 1.15 percent. As shown in Figure 12, Equation (24) compares favorably with the experimental results of Henry[7,8,10], the average deviation between the two curves being approximately 0.5 percent.

The variance in the experimental data was attributed to (a) difficulty in obtaining a uniform height of gate opening since the channel bottom in the vicinity of the gate was slightly concave, and (b) difficulty in maintaining the gate perfectly level as it was clamped to the sides of the flume. Both of these conditions resulted in minor discrepancy between the actual flow cross-section at the gate and that which was used in the computations.

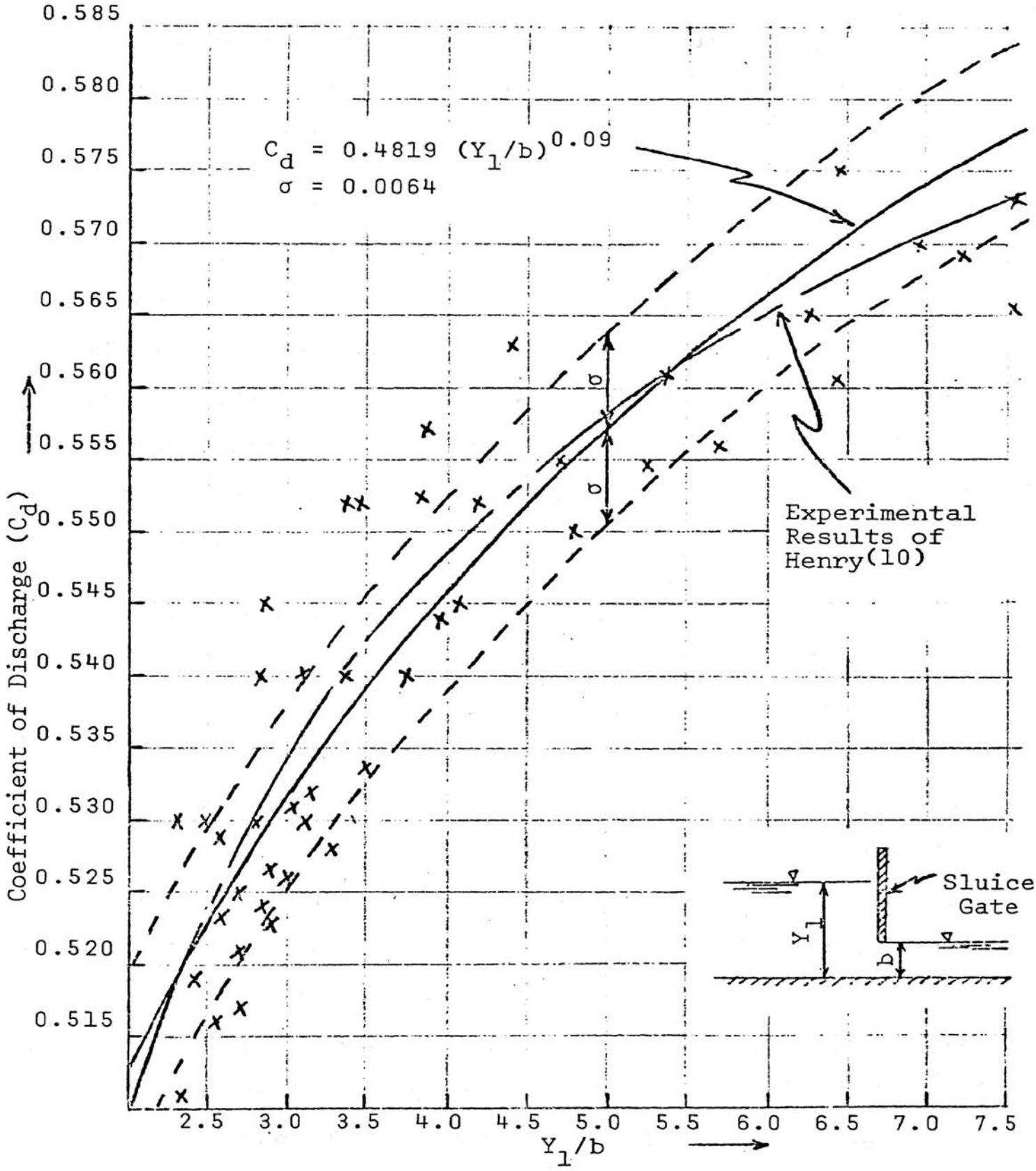

FIGURE 12. CORRELATION OF SLUICE GATE COEFFICIENT OF DISCHARGE (C_d) WITH DIMENSIONLESS RATIO (Y_1/b)

Flow measurements, throughout this investigation, were computed from Equation (7), where b and y_1 were measured and C_d was obtained from Figure 12.

B. Velocity Distribution

Velocity distribution energy coefficients (α) determined for representative nonaerated and aerated flows are given in Table I. The average α for nonaerated flow was 1.23 as compared to 1.27 for aerated flow. According to Chow[7] α for nonaerated flow varies from about 1.03 to 1.36 for straight prismatic channels, with smaller channels tending toward the higher value.

The "isovels" (contours of equal velocity) obtained for representative nonaerated flows, as shown in Figure 13, compare with those shown in hydraulic texts[7,8,9] for channels of rectangular cross-section. However, the region of maximum velocity was depressed farther below the water surface as the mean velocity increased for flows having similar width-depth ratios. This tendency was attributed to the fact that secondary flow, flow in a direction perpendicular to the main flow, became more pronounced as the discharge increased. Increased discharge resulted in higher inlet turbulence which in turn tended to cause a slight increase in flow depth on one side of the inlet. This condition caused the main flow to travel along the flume in a single spiral motion producing secondary flow[7].

TABLE I

VALUES OF THE VELOCITY DISTRIBUTION ENERGY COEFFICIENT (α) AS DETERMINED FOR SOME REPRESENTATIVE NONAERATED AND AERATED FLOWS

Type of Flow	Velocity (FPS)	α	Average α
Nonaerated	0.6	1.15	
Nonaerated	1.0	1.23	1.23
Nonaerated	1.0	1.24	
Nonaerated	0.5	1.31	
Aerated	0.6	1.32	
Aerated	0.9	1.27	1.27
Aerated	0.5	1.25	
Aerated	0.9	1.25	

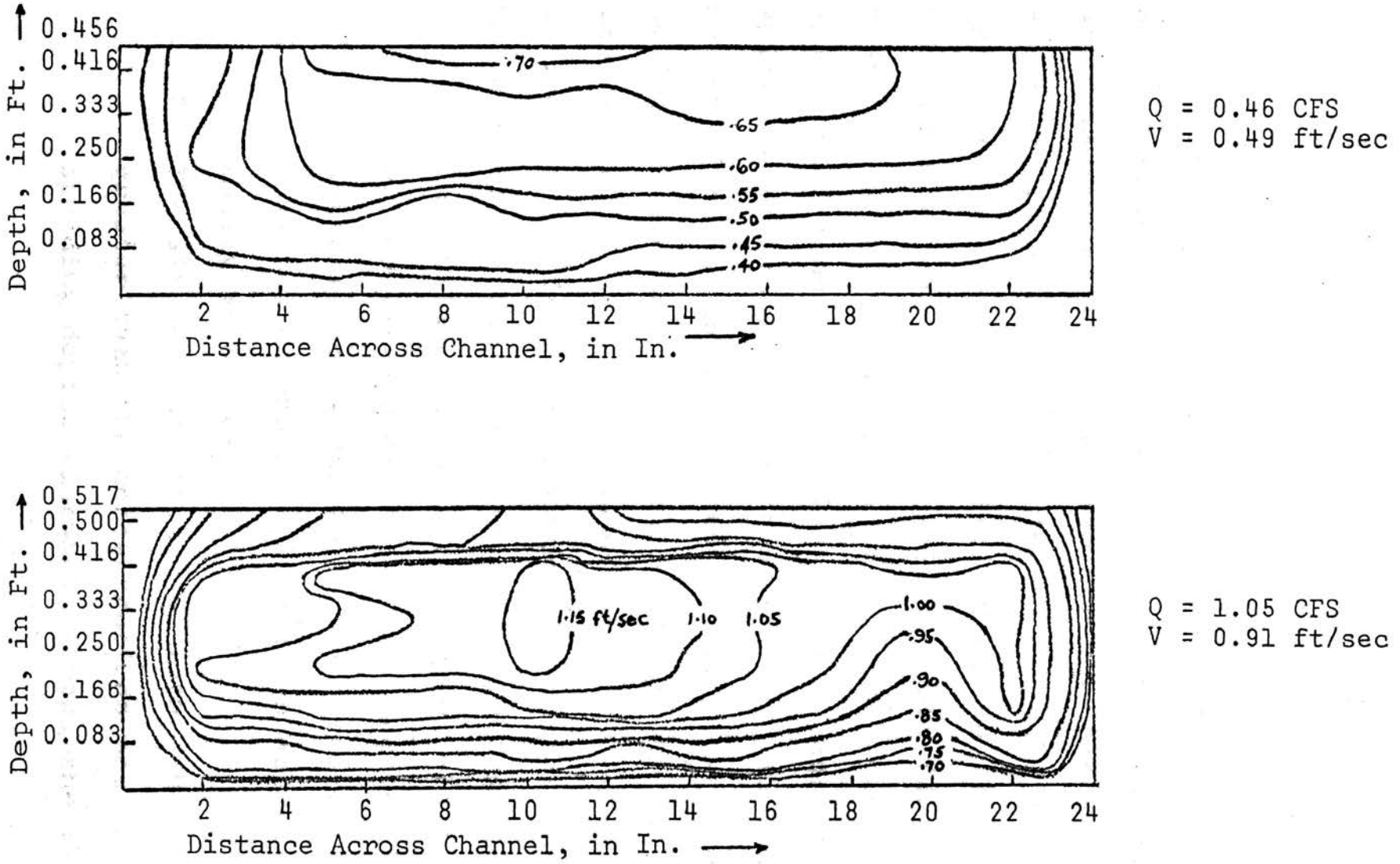

FIGURE 13. ISOVELS FOR SOME REPRESENTATIVE NONAERATED FLOWS

Isovels for representative aerated flows are shown in Figure 14. When compared with those of nonaerated flows of similar flow rate, it became apparent there were two regions of maximum velocity located on either side of the flow section generally 2 to 4 inches from the channel sides. In nonaerated flow in rectangular channels of small reach, secondary flow occurs since the flow develops along the channel in a single spiral motion[7]. In this type of flow there is one center of maximum velocity. When the flowing water is subjected to compressed air injected into flow along the channel bottom, the single spiral motion becomes a double spiral motion as upward moving air jets cause the single spiral motion to split into two spirals. This occurs at the center of the channel where the spiral flow is essentially horizontal and has no vertical component to resist the upward moving air jets. The conclusion that a double spiral motion results from the injection of compressed air along the channel bottom is based on the following observations:

1. The surface of the aerated flow, which was comprised largely of air bubbles, was observed to move laterally outwards from the center of the channel towards the channel sides at an angle of approximately 45 degrees.
2. The air concentrations along the channel sides were greater than the concentrations measured at corresponding depths elsewhere across the flow-section.

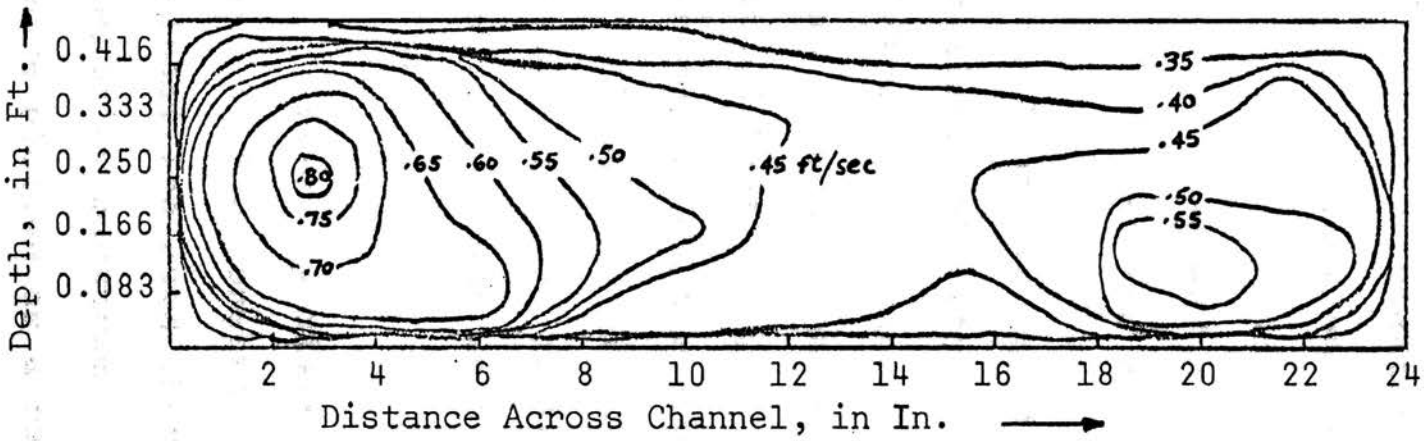

Q = 0.50 CFS
V = 0.47 ft/sec

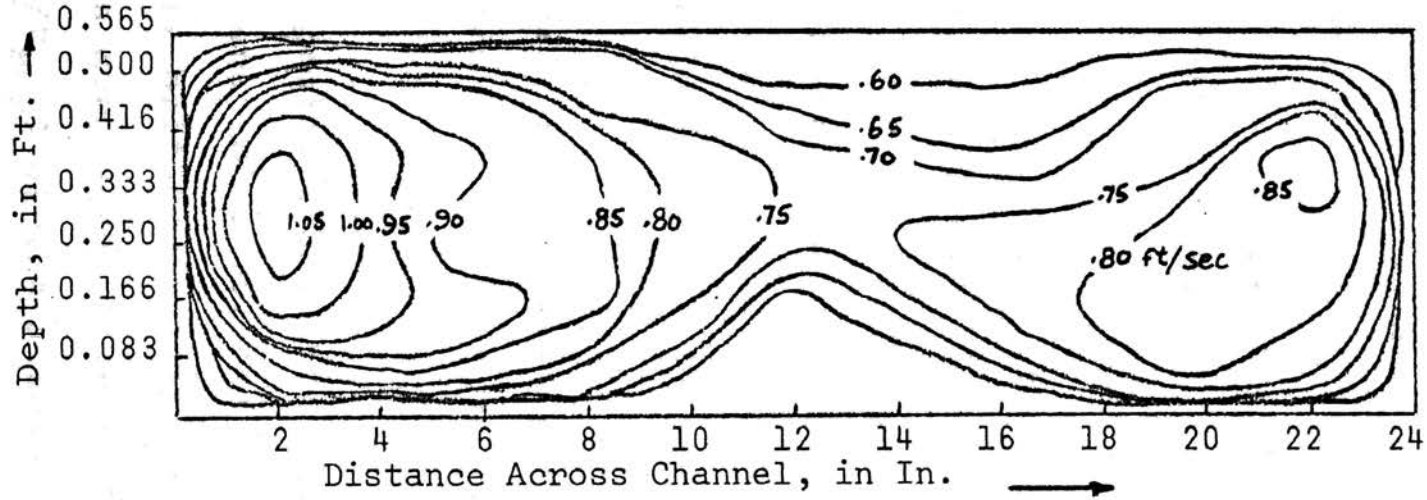

Q = 1.05 CFS
V = 0.71 ft/sec

FIGURE 14. ISOVELS FOR SOME REPRESENTATIVE AERATED FLOWS

Thus, at the channel walls, the upward movement of the air bubbles was opposed by the double spiral motion of the flowing water, which moved vertically downward in the vicinity of each channel wall. This caused the air bubbles to remain in the water for a longer period of time, resulting in concentrations of greater magnitude than elsewhere in the flow-section. At all other regions in the flow-section, the flowing water either helped the bubbles to ascend or did not directly oppose their ascension to the surface.

From Figure 14, it was also apparent that the region of maximum velocity of the aerated flow was depressed farther below the surface than that of the nonaerated flow. This was more noticeable at the lower rates of flow. It was reasoned that the greater depression of the regions of maximum velocity for the lower rates of flow was due to the fact that the intensity of secondary flow was not dependent upon the flow velocity, as in the case of nonaerated flow, but was only dependent upon the extent of aeration of the channel flow.

Velocity distribution profiles are shown in Figures 15 and 16 for nonaerated and aerated flows, respectively. The velocities used therein were arithmetic averages of point velocity measurements taken across the flow section. These were plotted as a ratio (V/V_{max}) of the average velocity (V)

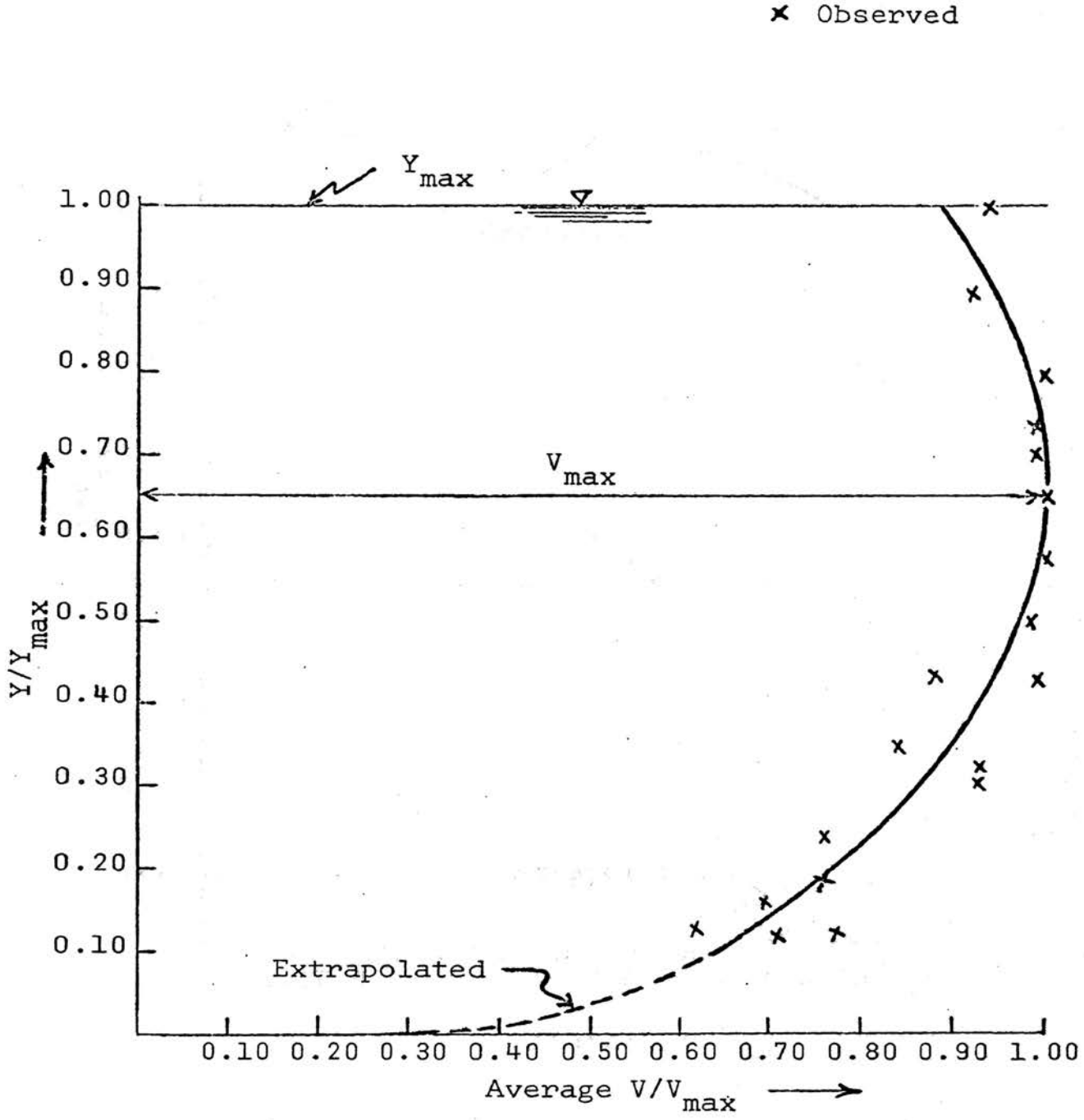

FIGURE 15. TYPICAL VELOCITY PROFILE FOR NONAERATED FLOW

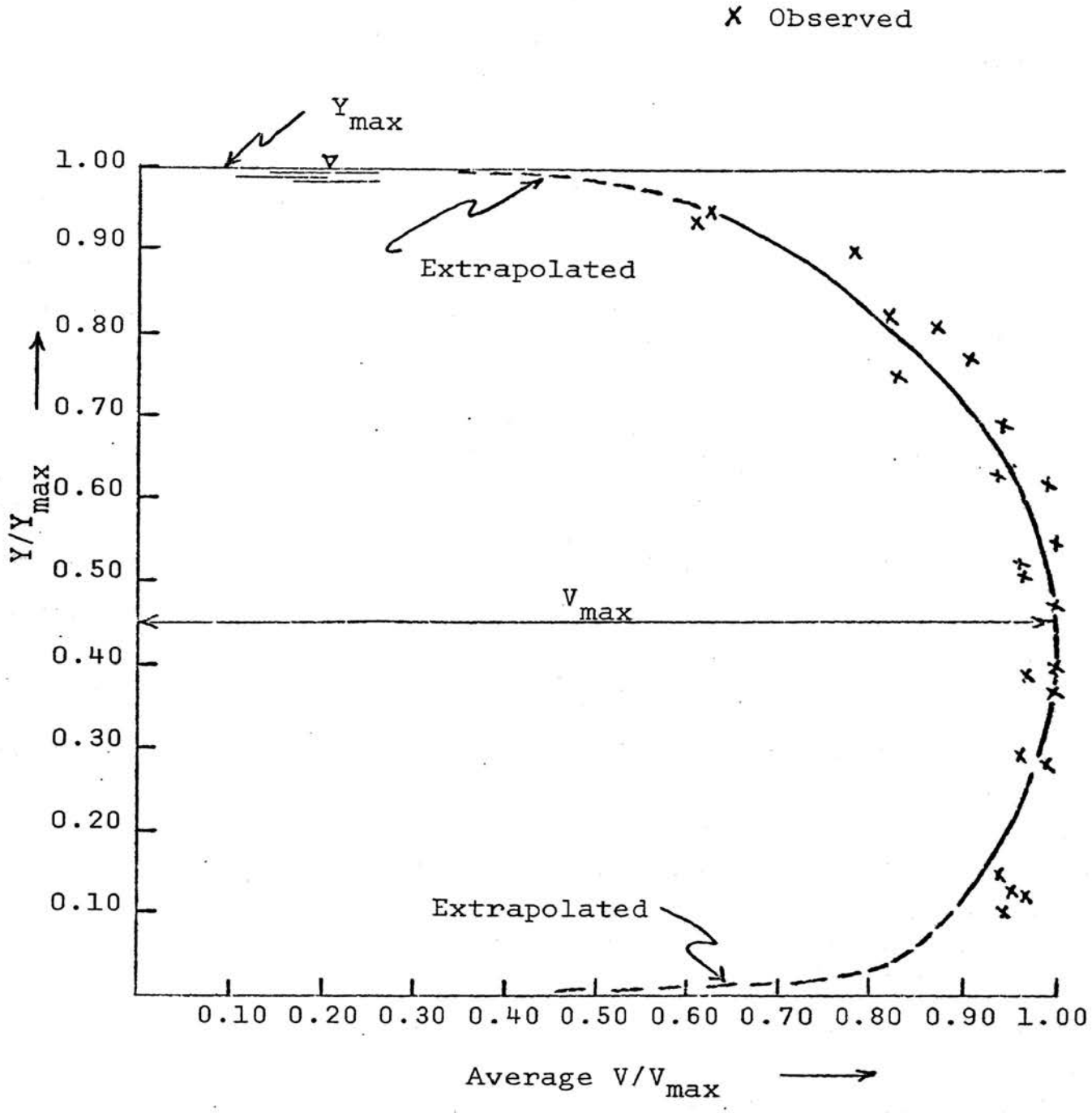

FIGURE 16. TYPICAL VELOCITY PROFILE FOR AERATED FLOW

at any depth to the simultaneous maximum velocity (V_{max}). The depth of flow was plotted as a ratio (y/y_{max}) where y was the depth of flow at which a particular velocity was measured and y_{max} was the maximum depth of flow associated with that particular velocity and depth measurement. The apparent scatter of data points was the result of combining several flow rates together. This was done in order to present velocity distribution trends for nonaerated flow as compared to aerated flow.

The velocity distribution profile for nonaerated flow was found to agree with typical velocity profiles for channels of similar width-depth ratios, as presented in hydraulic texts[7,8,9].

The velocity distribution profile for the aerated flow differed noticeably from that of the nonaerated flow. Noticeable variations are:

1. The point of maximum velocity of the aerated flow was depressed farther from the surface than in the nonaerated flow. The maximum velocity of the aerated flow was located at 45 percent of the depth of flow as compared with 65 percent of depth for the nonaerated flow.
2. The velocity decreased at a much greater rate as the surface was approached. The surface velocity of

nonaerated flow was about 90 percent of V_{max}. This compared with a velocity of 70 percent of V_{max} for the aerated flow; this velocity was measured at 90 percent of the depth of flow in the region just beneath the bubble layer.

The variations were attributed to the retarding effect of the "bubble layer" which comprised approximately 15 percent of the depth of flow. Although the Price pygmy current meter was ineffective in measuring the velocity of the bubble layer, it was visibly apparent that the bubble layer was traveling at a much lower velocity relative to the adjacent lower region containing discrete air bubbles. Thus, the bubble layer formed a fourth surface causing the open-channel flow to approach that of a closed conduit. This is evident from the similarities between the velocity profile of Figure 16 and that of a pipe flow velocity profile where the velocity asymptotically approaches zero at the pipe wall.

Although the preceding analysis was based on relative velocities in aerated and nonaerated flow and is thereby valid, a word of explanation is warranted concerning the absolute accuracy of velocity measurements. It was found that the mean velocity (V) computed from the flow rate (Q) divided by the flow cross-section (A) was in the range of 10 to 20 percent greater than that computed by Equation (10) from the point velocity measurements (v) across the flow

section. This discrepancy may have been due to the following factors:

1. The accuracy of the Price pygmy current meter was effected by the relative shallow and narrow channel in which it was used. The proximity of the channel bottom, sides, and surface may have produced an interference with the revolving of the meter cups as compared to its calibration which took place in a wider and deeper channel.
2. The size of the pygmy meter prevented velocity measurements near the channel sides and bottom. This necessitated the approximation of the velocity distribution in these areas, which may have contributed as much as 5 percent of the total discrepancy between the methods of determining the mean velocity (V).
3. The rising air bubbles may have interfered with the proper turning of the meter cups.

C. Air Concentration

The measured air concentration (c), of the aerated flow represented the average ratio of air volume to water volume flowing between the two electrodes of the resistance probe during a time interval. The air concentrations were determined for various aerated flows at selected grid points across the flow-section. These were plotted, and "isocons" (contours of equal air concentrations) were determined.

Typical isocons are shown in Figure 17. Maximum air concentrations were obtained in the vicinity of the surface in a region previously referred to as the bubble layer. Regions of minimum air concentration in the isocons were noticed to usually coincide with the regions of maximum velocity in corresponding isovels.

Utilizing a planimeter and Equation (11), the mean air concentration ($\overline{c}$) of a flow section was determined from an isocon. Mean air concentrations ($\overline{c}$) at two flow sections, one upstream at station 26.30 and the other downstream at station 8.25, were averaged to determine the mean concentration ($\overline{c}$) of a particular rate of aerated flow. As shown in Figure 18, the correlation of $\overline{c}$ with the mean depth of flow (y_m) along the reach of aerated flow indicated that $\overline{c}$ decreased as the depth increased. This trend was attributed to the fact that the air injected into the flowing water from the centrifugal blower remained essentially constant for a particular type of aerated flow (maximum air or minimum air), and was therefore independent of the depth of flow. Hence, a greater depth of flow would result in a decrease in $\overline{c}$ (the ratio of the volume of entrained air to the volume of flow).

The mean air concentration ($\overline{c}$) can also be used to define the aerated flow conditions (minimum air and maximum air) as used in this investigation. The two flow conditions

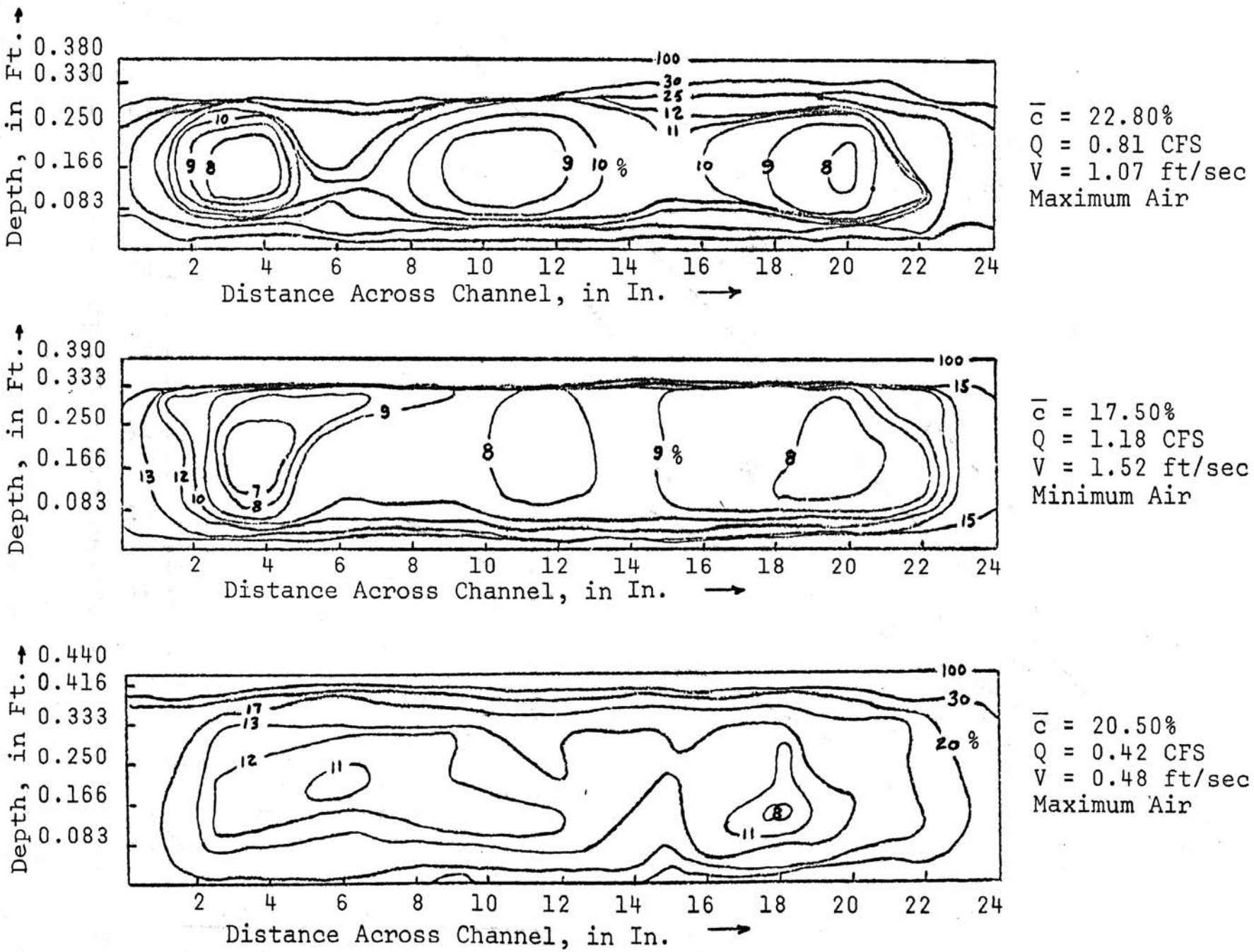

FIGURE 17. ISOCONS FOR SOME REPRESENTATIVE AERATED FLOWS

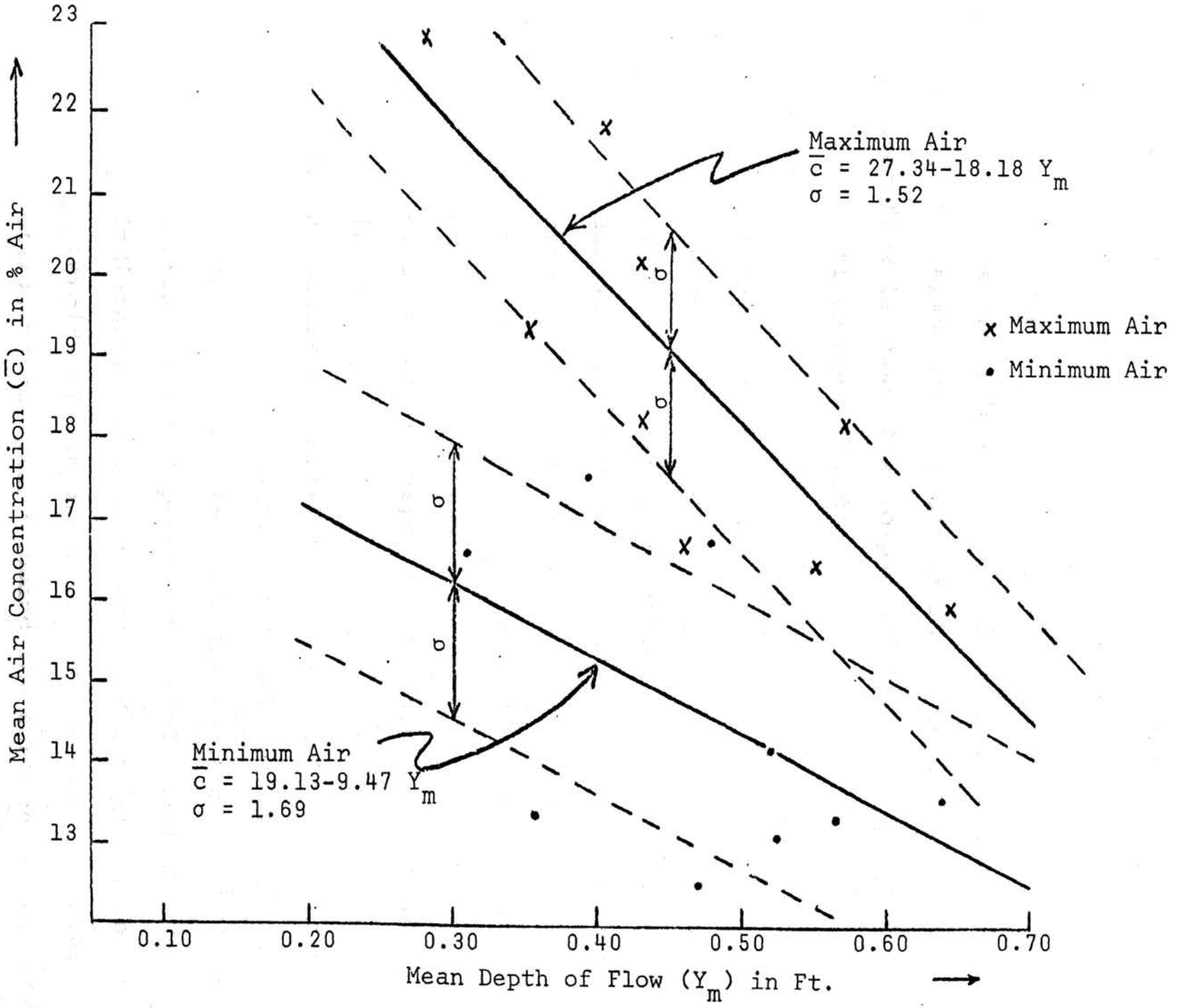

FIGURE 18. CORRELATION OF MEAN AIR CONCENTRATION ($\bar{c}$) WITH MEAN DEPTH OF FLOW (Y_m)

are related by an air concentration ratio (C_R) which is the ratio of $\overline{c}$ for maximum air to $\overline{c}$ for minimum air. C_R varies with depth of flow as shown in Figure 19.

Average air concentration (c_A) profiles for various aerated flows of maximum air and minimum air are shown in Figure 20. Also, the air concentration profile of self-aerated flow is shown for comparison[14]. The air concentration profiles were divided into the following three regions:

1. An "air-jet" region, as shown in Figure 21, at the channel bottom, comprising approximately 15 percent of the total depth of aerated flow for the maximum air and approximately 5 percent for the minimum air; here the compressed air entered the flowing water through the equally-spaced 0.040 inch diameter holes in the channel bottom; the jets were somewhat cylindrical in shape with a diameter of about 3/8 inch;
2. A "discrete bubble" region, as shown in Figure 22, comprising approximately 70 percent of the total depth of the aerated flow for maximum air and approximately 80 percent for minimum air; here individual bubbles, shaped as deformed oblate spheroids of varying size (1/4 to 3/8 inch diameter), moved upward toward the surface of the water in a more or less downstream direction depending on

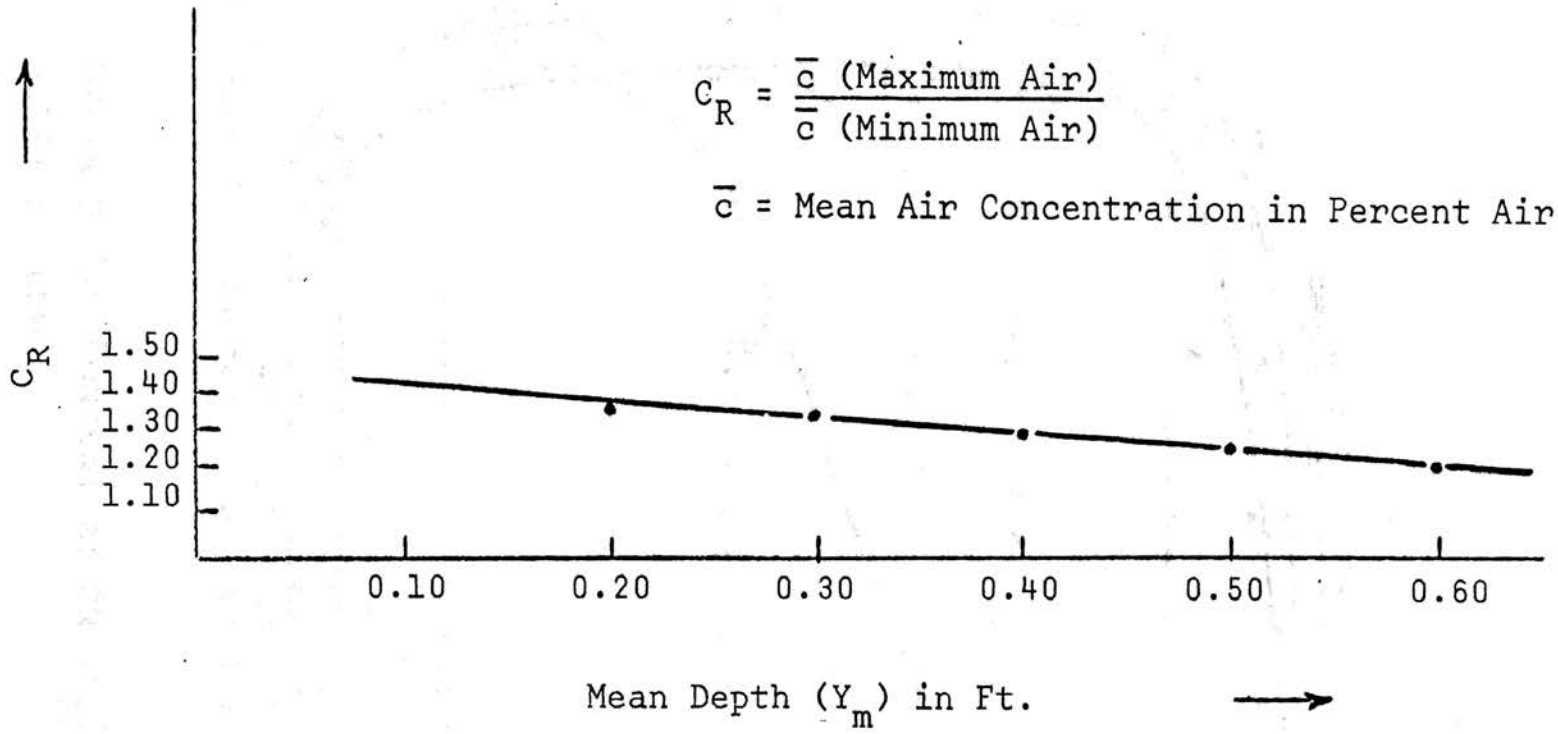

FIGURE 19. CORRELATION OF C_R WITH MEAN DEPTH OF FLOW (Y_m)

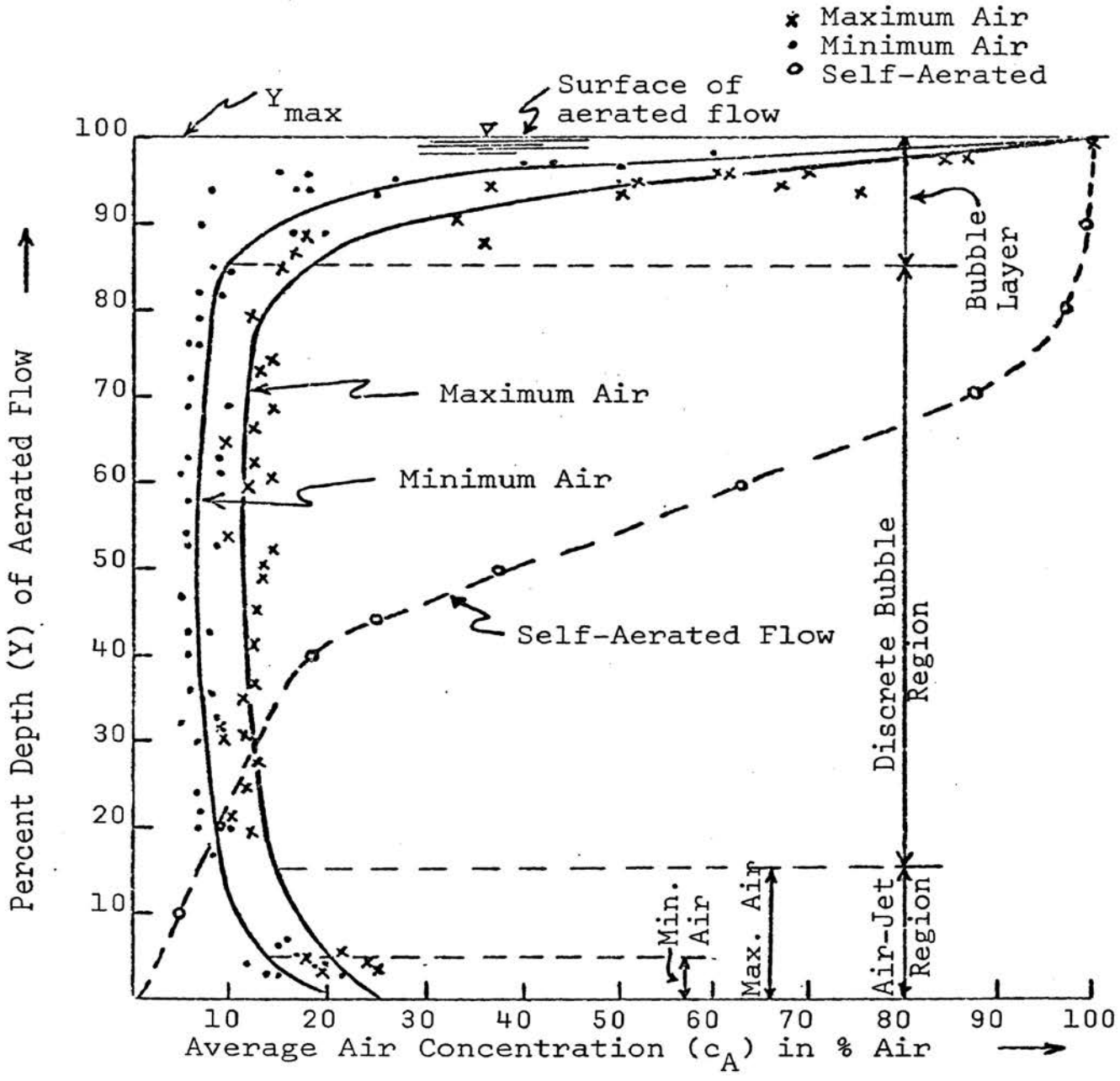

FIGURE 20. AVERAGE AIR CONCENTRATION (c_A) PROFILES OF AERATED FLOW

FIGURE 21. "AIR-JET" REGION OF AERATED FLOW

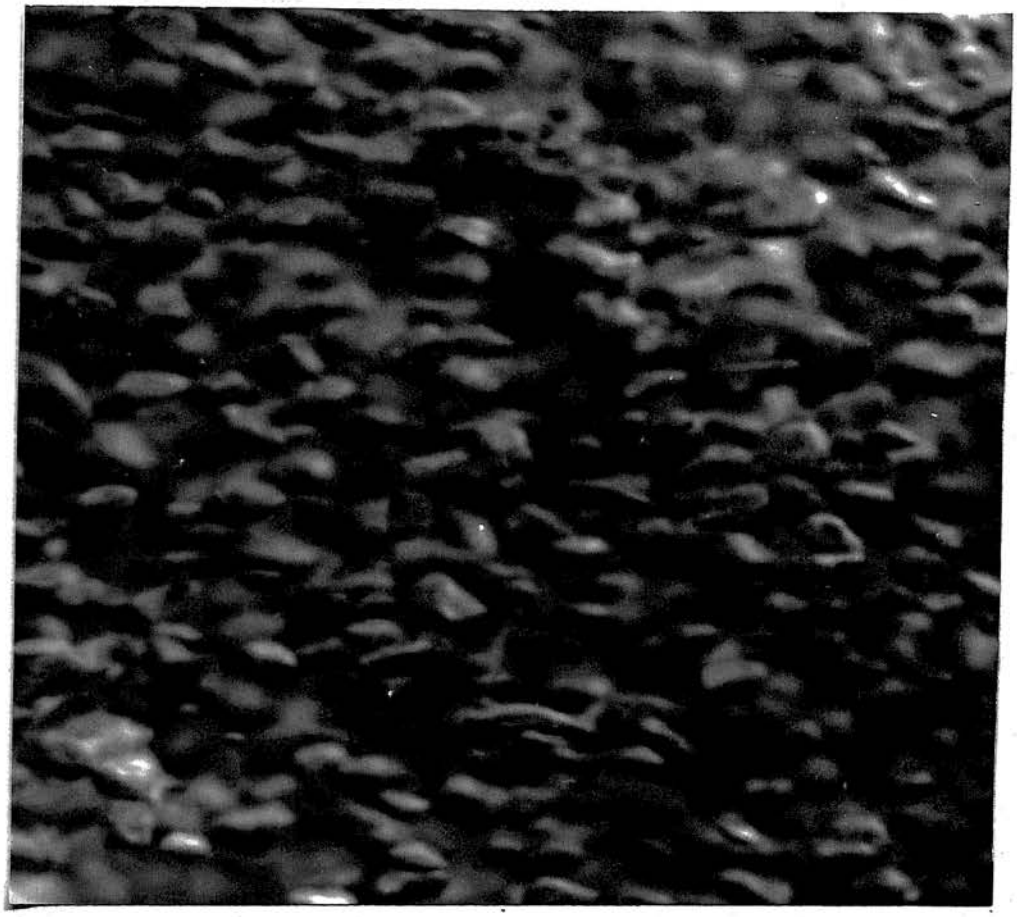

FIGURE 22. "DISCRETE BUBBLE" REGION OF AERATED FLOW

the velocity of the flowing water; the bubbles were formed as each air-jet broke apart due to the resistance of the water to the upward motion of the jet; the air concentration (c) remained essentially constant throughout this region; and

3. A bubble layer region, as shown in Figure 23, near the water surface, comprising approximately 15 percent of the total depth of aerated flow; here, the upward motion of the bubbles from the discrete bubble region was significantly reduced due to the delaying effect of surface tension upon their escape into the overlying atmosphere; this resulted in considerable coalescence of the individual bubbles into larger bubbles; the air concentration (c) in this region asymptotically approached the value of 100 percent corresponding to the free surface of the aerated flow.

D. Bulking

The presence of the entrained air bubbles in the flowing water resulted in an increase in the depth of flow. The ratio of this increase in depth of aerated flow to the depth of a corresponding nonaerated flow was defined as "bulking" (B). Linear correlations of B versus the depth (y) of nonaerated flow are shown in Figure 24 for the two types of aerated flow, maximum air and minimum air respectively.

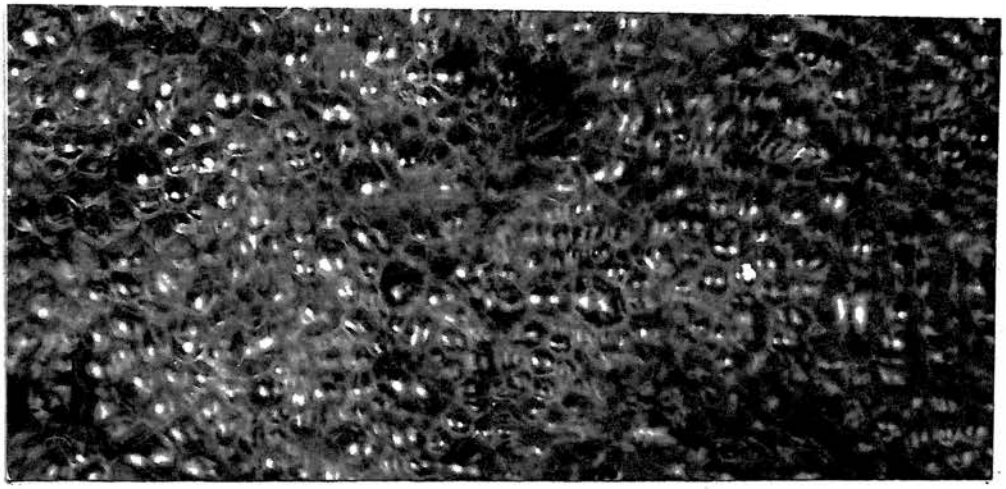

TOP VIEW

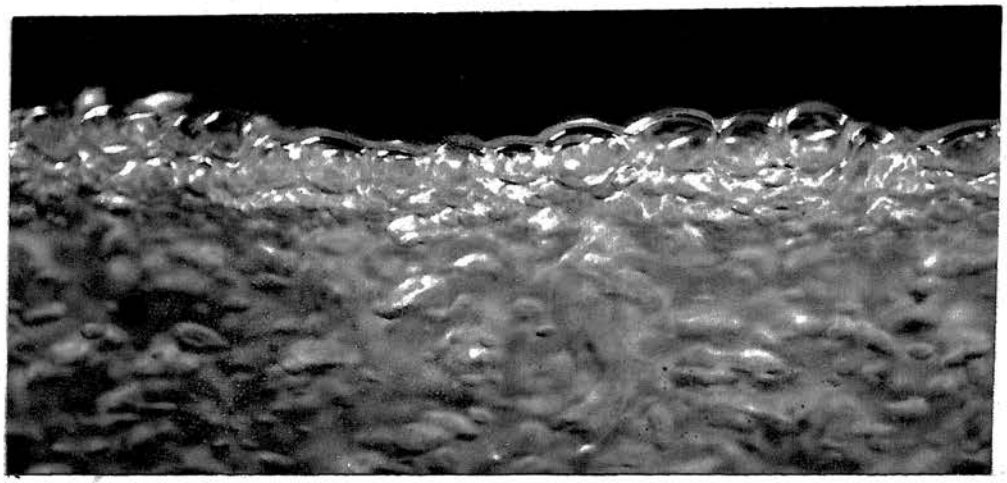

SIDE VIEW

FIGURE 23. "BUBBLE LAYER" REGION OF AERATED FLOW

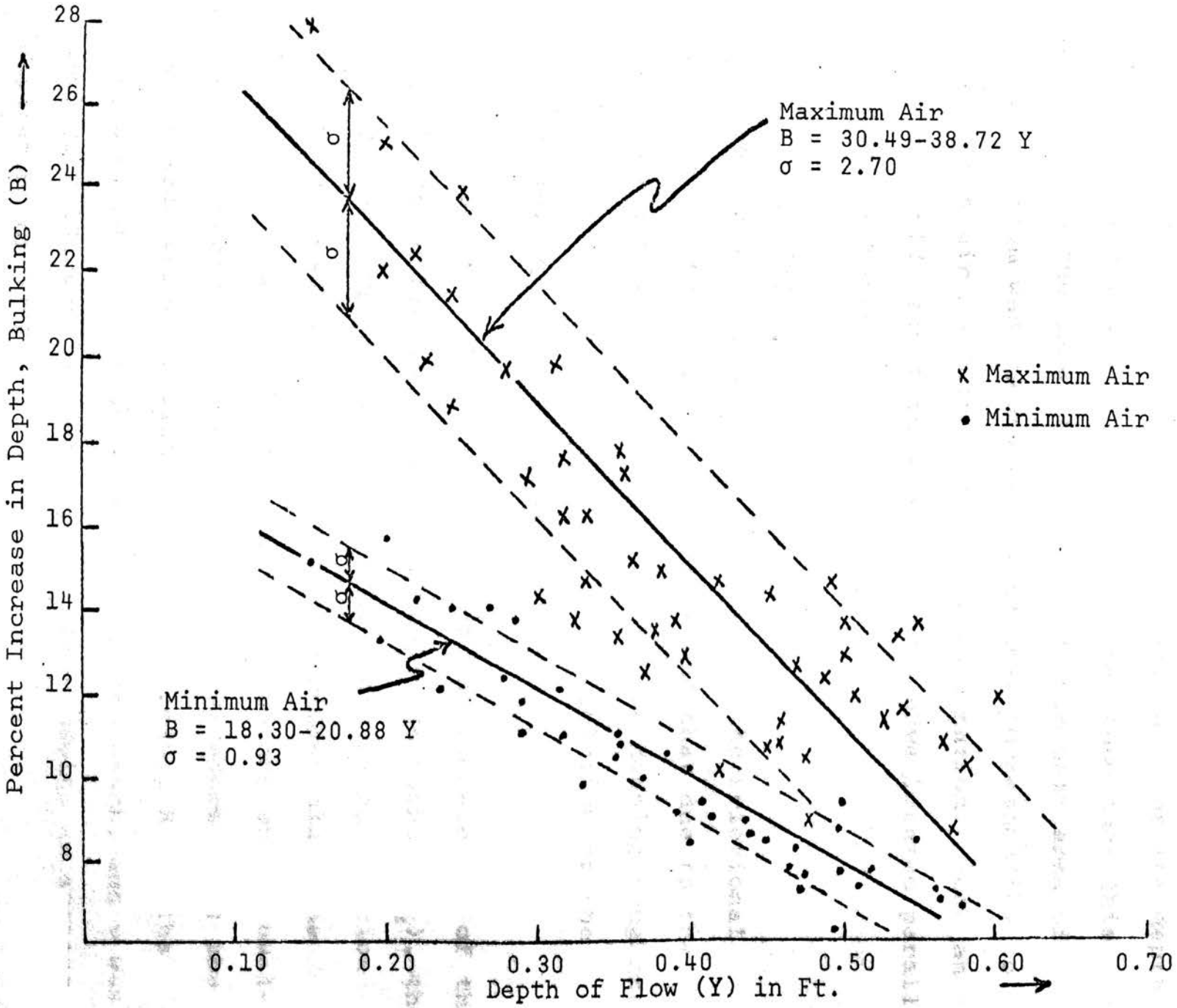

FIGURE 24. CORRELATION OF BULKING (B) WITH DEPTH OF FLOW (Y)

The correlations revealed a significant decrease in B with increasing depth (y) such that the bulking effect appears to approach a level of insignificance as the depth approaches 1.0 foot. However, it is reasoned that this would not be the case if the air input per unit area of channel bottom was increased beyond that corresponding to the maximum air condition of this investigation. Such an increase would result in a correlation curve located parallel to and above those in Figure 24.

E. Flow Retardance

The combined flow retardance due to the frictional resistance at the channel boundaries and that due to the injected air was evaluated in terms of the Manning roughness coefficient (n), utilizing an iterative solution of the differential equation of varied flow.

In order to utilize the conventional correlation of the Darcy friction factor (f) with the Reynolds number (R_e), the Manning n was expressed as the Darcy f utilizing Equation (22) where R was the average hydraulic radius along the channel for nonaerated flow. The Reynolds number was evaluated for nonaerated flow by Equation (23) where V was the average mean velocity along the channel reach, R was the average hydraulic radius along the channel reach, and ν was equal to 0.0000096 centistokes for water having an average temperature of 77°F.

The correlation of f with R_e is shown in Figure 25. The Blasius and Prandtl-von Kármán equations for a smooth conduit are shown for comparative purposes. The curve identified as nonaerated indicates the variation of f with R_e for the condition of nonaerated flow while those identified as minimum air and maximum air indicate the variation of f with R_e for the two aerated flow conditions which were previously defined. It is evident from Figure 25 that the four curves are approximately parallel and that the friction factor (f) increases as the Reynolds number decreases. Also, it is apparent that for a given Reynolds number, f substantially increases when the flow is aerated. The f of the aerated flow (minimum air) is approximately 160 percent that of the nonaerated flow, and the f of the aerated flow (maximum air) is approximately 215 percent that of the nonaerated flow. The average value of f for the nonaerated flow is 0.025 which is within the range of values given in hydraulic texts[7,8] for channels constructed of material similar to that of the experimental channel (plexiglass). The f curves for the two aerated flows tend to follow the same relationship to the Blasius and Prandtl-von Kármán curves[7] as those that Bazin, Kirschmer, and others found for channels of various degrees of roughness.

Figure 26 shows a correlation of the Manning n with the parameter VR, where V is the mean velocity and R is the mean hydraulic radius for nonaerated flow. The n of the aerated

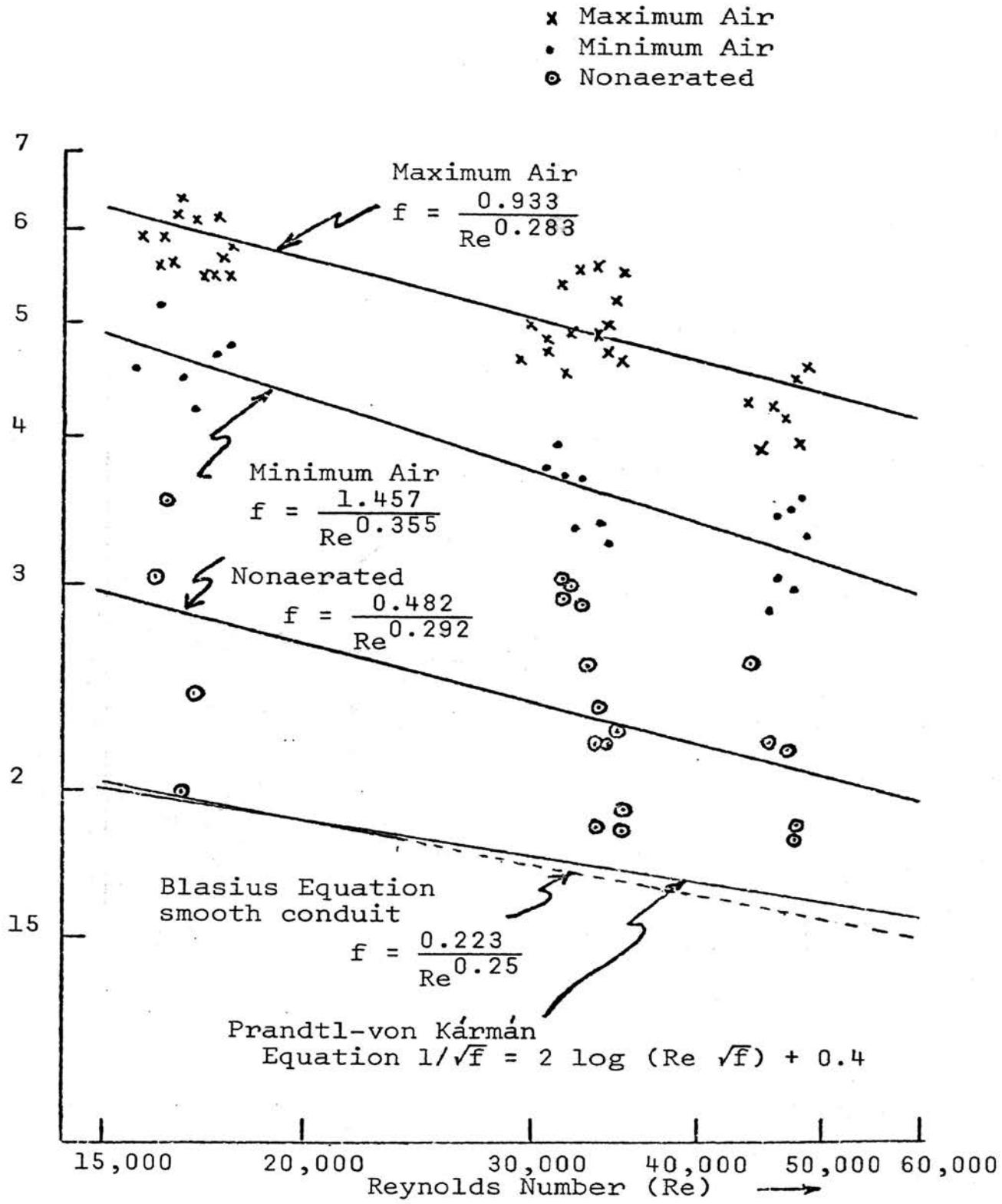

E 25. CORRELATION OF DARCY FRICTION FACTOR (f) WITH REYNOLDS NUMBER (Re)

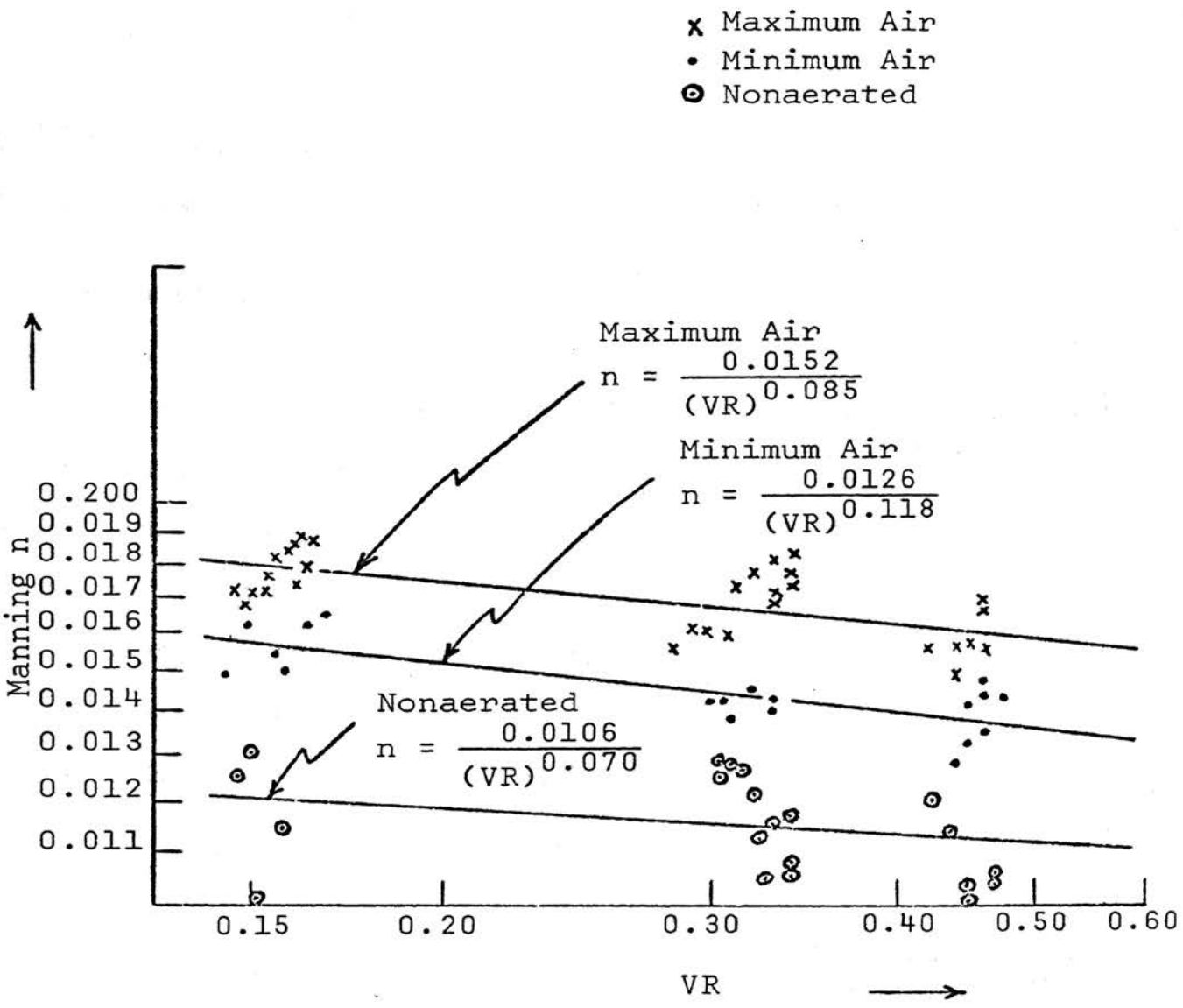

FIGURE 26. CORRELATION OF MANNING n WITH VR

flow (minimum air) is approximately 125 percent that of the nonaerated flow, and the n of the aerated flow (maximum air) is approximately 145 percent that of the nonaerated flow. The average value of n for the nonaerated flow is 0.0115 which is within the range of values given in hydraulic texts[7,8] for channels constructed of material similar to that of plexiglass.

The correlation of n with VR is used for open channels having a grass lining[7]. As will be pointed out later, there are some aspects of aerated flow due to the injection of compressed air which resembles the flow retardance characteristics of a grass-lined channel and it is for this reason that Figure 26 is included. The n curve for maximum air is parallel to and approximately 30 percent of the magnitude of a n curve, given by Chow[7], for grass-lined channels having a very low vegetal retardance.

Since, in this investigation, the velocity and depth of flow were the two variables determining the Reynolds number, it was decided that separate correlations of n with depth and with velocity would provide additional insight into the nature of the increase in n for aerated flow.

Correlations of n with the mean velocity (V) along the channel for nonaerated flow and the two conditions of aerated flow are shown in Figure 27. The n curves for minimum air and maximum air parallel each other and indicate a substan-

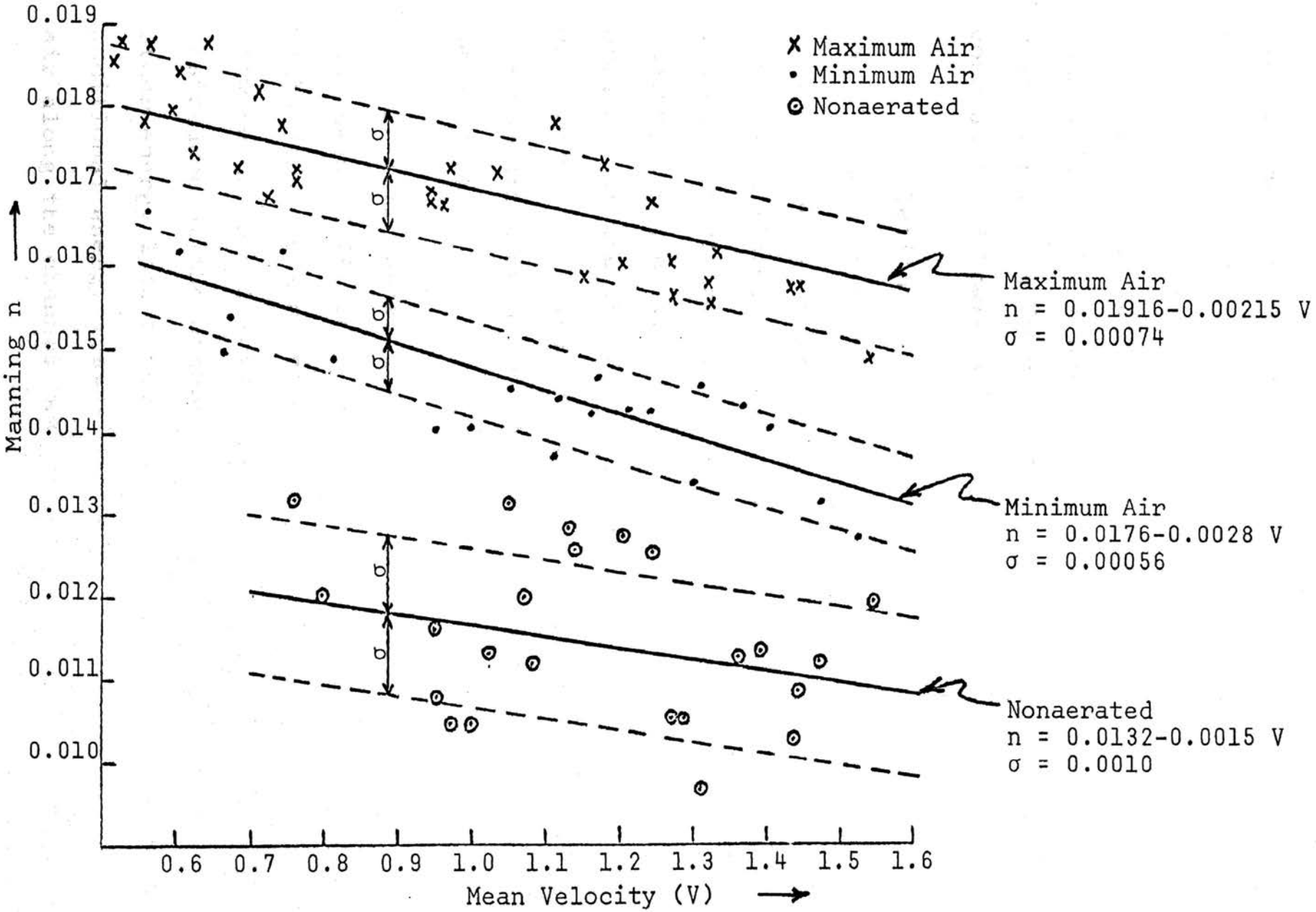

FIGURE 27. VARIATION OF MANNING n WITH MEAN VELOCITY (V)

tial increase in n with a decrease in the velocity. Although this same trend is noted for the n curve for nonaerated flow, the slope is 50 percent less and the considerable scatter of data points suggests that the trend in this case is not very meaningful. The tendency toward a decrease in the Manning n with an increase in velocity of aerated flow agrees with the conclusion of Townsend[5].

Correlations of n with the mean depth of flow (y_m) along the channel for nonaerated flow and the two conditions of aerated flow are shown in Figure 28. Here, the n curves for nonaerated flow indicate a substantial increase in n with a decrease in depth. This agrees with present hydraulic theory, i.e., as the depth decreases the flow disturbances produced at the channel boundaries influence a greater percentage of the total flow. The n curves for minimum air and maximum air show no relationship between n and depth for aerated flow.

In this investigation it was assumed that the Manning roughness coefficient (n) or the Darcy friction factor (f) would serve as a means of evaluating not only the degree of flow retardance (energy losses) attributed to frictional resistance at the channel boundary but also those due to other energy losses such as secondary flow, as well as any additional energy losses due to the injection of compressed air along the channel bottom. Thus, for the nonaerated flow

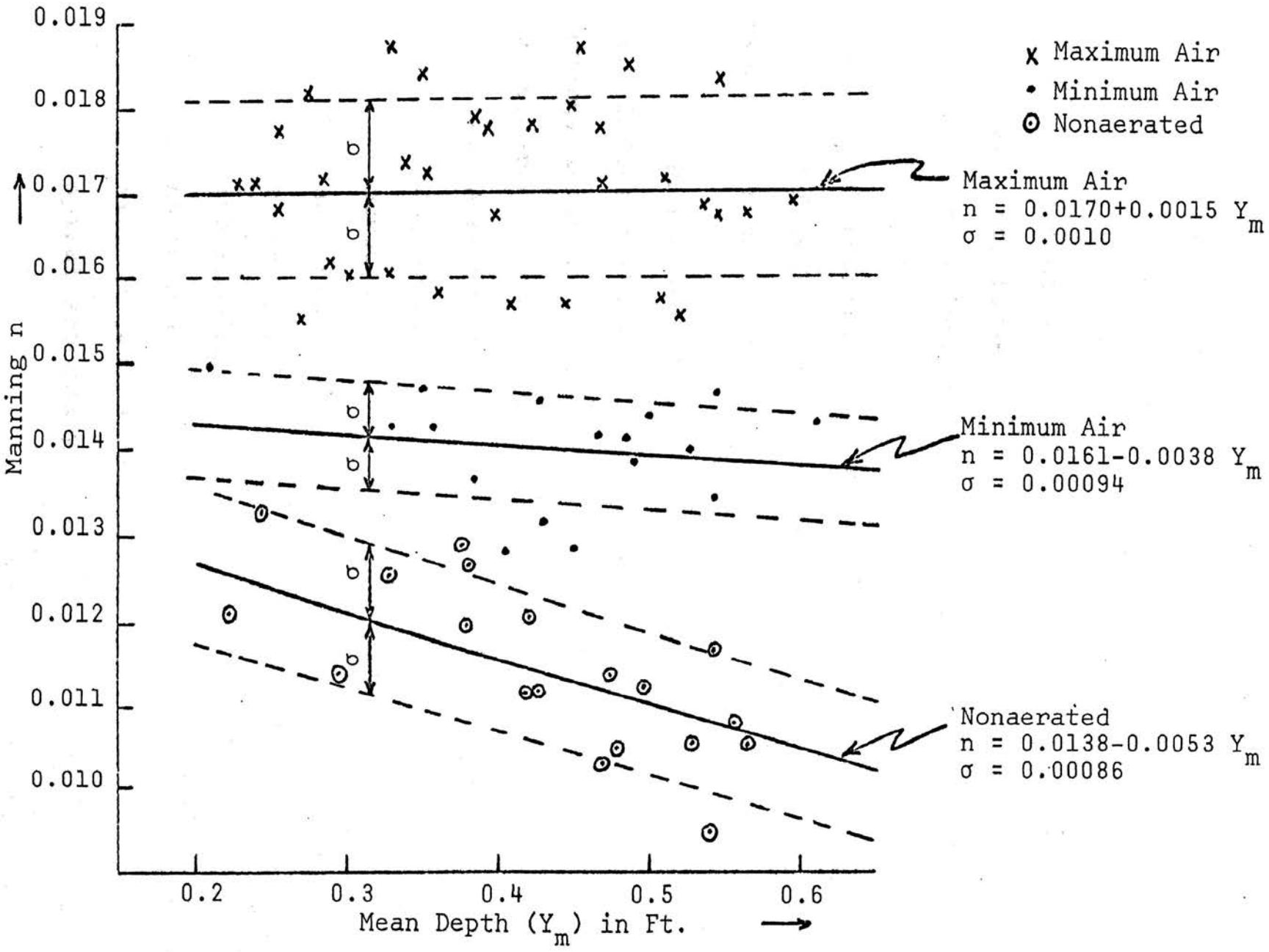

FIGURE 28. VARIATION OF MANNING n WITH MEAN DEPTH OF FLOW (Y_m)

of this investigation, the factors causing flow retardance were:

1. Frictional resistance along the channel boundaries (the bottom and the sides);
2. Secondary flow[7] due to the single spiral flow prevalent in rectangular-shaped channels; and
3. Eddy losses[7] produced in a varied flow of decreasing velocity such as the type of varied flow resulting from a channel restriction, e.g., a sluice gate.

Frictional resistance at the channel boundary was the primary cause of flow retardance while secondary flow and eddy losses were minor contributors.

When the same flow was subjected to diffused compressed air injected along the channel bottom, the increase in the energy losses, as noted by an increase in the Manning n, was considered to be due to the following factors:

1. A restriction of the flow area in the air-jet region due to a portion of the flow area being occuppied by the air-jets;
2. An energy loss resulting from a disturbed flow due to the air-jets opposing the horizontal movement of the flowing water;
3. An increase in energy loss due to a greater intensity of secondary flow as evidenced by the double spiral secondary flow induced by the injected air;

4. An increase in the boundary frictional resistance due to the addition of a fourth boundary surface, the bubble layer that floated on top of the flowing water; and
5. Eddy losses and flow disturbances produced by the free-floating discrete air bubbles rising through the flowing water.

Referring to factors (1) and (2), the influence of the air-jets on the flowing water somewhat resembles that due to a grass lining of an open channel. In each case, the flow area is restricted and the flow is disturbed by the projection of the air-jet or blade of grass into the flowing water. As the flow velocity increases the air-jets or blades of grass, as the case may be, are bent in the direction of the flowing water, and the ratio of restricted flow area to total flow area is decreased. This would seem to account, at least in part, for the decrease in the Manning n with an increase in velocity as was noted in Figure 27.

Referring to factors (3) and (4), the fact that secondary flow exists and the nature of the bubble layer were previously discussed in the section entitled Velocity Distribution. It is also apparent that each would produce energy losses and thus contribute to the apparent increase in the Manning n for aerated flow.

Referring to factor (5), it is apparent that flow disturbances are produced as the discrete air bubbles travel upward towards the surface through the flowing water, since this upward motion opposes the horizontal movement of the flowing water. Also, due to viscosity, a wake containing eddies is created as each bubble travels upward. Thus energy losses would arise out of the flow disturbance and eddies created by the ascending bubbles.

Referring to Figures 25 and 26, it is reasonable to assume that as the available air pressure increases above that which was used in this investigation to produce maximum air, the f or n curve, as the case may be, would be located above and parallel to those in Figures 25 and 26. This would be due to the air-jets, whose extent of projection into the flowing water is dependent upon the magnitude of the pressure differential existing between that inside the air diffusion compartments and the static pressure due to the depth of flowing water in the channel. Thus, the greater the available air pressure, the greater would be the retarding effect of the air-jets upon the open-channel flow.

This investigation was confined to relatively shallow depths of flow. It would be expected that at greater depths the relative importance of factors (1) and (2) would diminish while the importance of remaining factors (3), (4), and (5) would remain essentially constant. It is therefore

anticipated that some decrease in the Manning roughness coefficient (n) due to aeration would be expected at considerably greater depths of flow. This relationship would be similar to that for nonaerated flow where n has been shown to decrease as the depth increases.

F. Effect of Slope

The preceding data was obtained for two conditions of channel slope, (a) a steep slope of 0.004975 ft/ft and (b) a mild slope of 0.00100.

There was no apparent effect on the following due to a change in channel slope:

1. The coefficient of discharge (C_d) of the sluice gate;
2. The total mean air concentration ($\bar{c}$) and the average air concentration profiles; and
3. The extent of bulking of the aerated flows.

Hence, the data obtained from both slope settings of the flume were combined in the final analysis of the discharge, air concentration and bulking.

Concerning the data on flow retardance, only that which was obtained for the slope of 0.004975 was used. The data obtained for the slope of 0.0010 was not utilized due to its erratic nature, which was believed to be due to the accuracy of the depth measurements. The magnitude of probable error in the depth measurements was a significant percentage of the total measured headloss.

VII. CONCLUSIONS

The data obtained in this investigation provided an insight into some aspects of the hydraulic phenomena accompanying low-velocity, open-channel flow subjected to aeration by the injection of diffused compressed air. Several conclusions were drawn from the analysis of the data. These conclusions are offered subject to: (a) the range of flow depths, velocities, and air pressures which were studied, and (b) the geometry of the air diffuser system utilized in this investigation. The conclusions are:

1. The velocity distribution of open-channel flow is significantly altered when subjected to aeration. The maximum velocity for aerated flow occurs nearer the mid-point depth than for nonaerated flow; the bubble layer at the surface of aerated flow tends to produce a frictional resistance which causes the velocity to pronouncedly decrease as the surface is approached; the flow cross-section of aerated flow contains two centers of maximum velocity as compared to one for nonaerated flow.
2. Air injection tends to induce secondary flow of a double spiral pattern.
3. Aerated flow consists of three regions: (a) an air-jet region located near the channel bottom; (b) a

bubble layer region located at the surface, and (c) a discrete bubble region located in between the air-jet and bubble layer regions.

4. The air concentration is essentially constant in the vertical direction over that portion of the flow depth described as the discrete bubble region, and in the bubble layer region the air concentration asymptotically approaches 100 percent at the surface of the bubble layer.
5. An increase in depth defined as bulking results from the addition of compressed air to open-channel flow; the degree of bulking increases as the depth decreases and as the air content increases; for the air content studied in this investigation, bulking becomes insignificant as the depth approaches 1.0 foot.
6. When open-channel flow is subjected to aeration, there is a substantial increase in the flow retardance as a direct result of the aeration; the Manning roughness coefficient (n) for the aerated flow of this investigation was approximately 125 percent that of nonaerated flow for the case of minimum air and approximately 145 percent that of nonaerated flow for the case of maximum air; the Darcy friction factor (f) was approximately 160 percent that of nonaerated flow for the case of minimum

air and approximately 215 percent that of non-aerated flow for the case of maximum air.

7. In aerated flow, the Manning n or the Darcy f increases as the velocity of flow decreases and as the air pressure of the injected compressed air increases.

8. The increase in flow retardance resulting from the injection of compressed air along the channel bottom is due to the following qualitative factors:
   (a) Restriction of flow area in the air-jet region;
   (b) Disturbance of flow due to the air-jets;
   (c) Increase in secondary flow resulting from the aeration process;
   (d) Increase in boundary frictional resistance due to the bubble layer; and
   (e) Flow disturbances and eddy losses resulting from the ascension of discrete air bubbles to the surface.

9. Channel slope does not affect the air concentration or the bulking of the aerated flow of this investigation.

VIII. RECOMMENDATIONS FOR FUTURE RESEARCH

This investigation has merely touched upon the surface of the knowledge required to understand the complexities of aerated flow. Many more such investigations will be required if adequate understanding is to be achieved. The writer's recommendations for some further investigations are as follows:

1. Investigate the velocity distribution, air concentration, and flow retardance for aerated flow in which the range of air pressures and depths of flow are extended beyond those of this investigation.
2. Repeat No. 1 with different geometrical patterns of air injection.
3. Investigate the flow retardance of aerated flow at various channel slopes.
4. Investigate the velocity distribution of aerated flow utilizing a more precise method of velocity measurement than was used in this investigation, e.g., a hot film anemometer or SAF salt velocity meter[15].
5. Investigate the mechanics of bubble formation and the ascension paths of the bubbles, utilizing high speed photography.

6. Investigate the contribution to flow retardance due to frictional resistance at the bubble layer by using acetate spheres to approximate the air bubbles.
7. Investigate the velocity distribution in the air-jet region for different geometrical patterns of air injection and compare with velocities derived via potential theory.
8. Investigate the distribution and relative magnitude of the secondary flow induced by the aeration process.

BIBLIOGRAPHY

1. Lane, E. W., "Entrainment of Air in Swiftly Flowing Water," Civil Engineering, Vol. 9, p. 88, February 1939.

2. Straub, L. G. and A. G. Anderson, "The Distribution of Air in Self-Aerated Flow in Smooth Open-Channels," Hydraulic Laboratory Project No. 48, July 1955.

3. Straub, L. G. and A. G. Anderson, "Experiments in Self-Aerated Flow in Open-Channels," Proceedings, ASCE, Vol. 84, No. Hy7, December 1958.

4. Einstein, H. A. and O. Sibul, "Open Channel Flow of Water-Air Mixtures," Transactions, American Geophysical Union, Vol. 35, No. 2, p. 235, April 1959.

5. Townsend, D. W., "Loss of Head in Activated Sludge Aeration Channels," Proceedings, ASCE, Vol. 60, January 1934.

6. Thackwell, H. L., Discussion of "Loss of Head in Activated Sludge Aeration Channels," by D. W. Townsend, Proceedings, ASCE, Vol. 60, March 1934.

7. Chow, V. T., "Open-Channel Hydraulics," McGraw-Hill, New York, 1959.

8. Henderson, F. M., "Open Channel Flow," Macmillan, New York, 1957.

9. Rouse, H., "Fluid Mechanics for Hydraulic Engineers," Dover Publications, 1961.

10. Henry, R. R., Discussion of "Diffusion of Submerged Jets," by M. L. Albertson, Y. B. Dai, R. A. Jenson, and H. Rouse, Transactions, ASCE, Vol. 115, p. 687, 1950.

11. Lee, M., H. E. Babbitt, and E. R. Baumann, "Gradually Varied Flow in Uniform Channels on Mild Slopes," University of Illinois Engineering Experiment Station, Bulletin Series No. 404, University of Illinois, Urbana, Illinois, 1952.

12. Lamb, O. P. and J. M. Killen, "An Electrical Method for Measuring Air Concentration in Flowing Air-Water Mixtures," University of Minnesota, St. Anthony Falls Hydraulic Laboratory Technical Paper No. 10, Series B, March 1952.

13. Ezekiel, M., "Methods of Correlation Analysis," Wiley, New York, 1947.

14. Streeter, V. L., "Handbook of Fluid Dynamics," Open-Channel Flow by V. T. Chow, p. 24-57, McGraw-Hill, New York, 1961.

15. Straub, L. G., J. M. Killen, and O. P. Lamb, "Velocity Measurements of Air-Water Mixtures," Transactions, ASCE, Vol. 79, p. 207, May 1953.

APPENDIX

COMPUTER PROGRAM

FORTRAN IV DIGITAL COMPUTER PROGRAM

FOR SOLVING THE DIFFERENTIAL EQUATION OF

GRADUALLY VARIED FLOW

```
 1          DIMENSION AN(40),E(40),SF(40),ASF(40),DX(40),X(40)
 2          WRITE (3,300)
 3          S=0.004975
 4          READ(1,100)(AN(J),J=1,12)
 5       30 READ(1,600,END=999)   N
 6          READ(1,500,END=999)  Q
 7          READ(1,500,END=999)   (Y(K),K=2,N)
 8          DO 10 J=1,12
 9          DX(2)=0.
10          X(2)=0
11          DO 10 K=2,N
12          A=2.*Y(K)
13          RP=(A/(2.+2.*Y(K)))**1.333
14          V=Q/A
15          VH=(1.23*V*V)/64.4
16          SF(K)=(AN(J)*AN(J)*V*V)/(2.22*RP)
17          E(K)=Y(K)+VH
18          IF(K-2)1,1,2
19        1 WRITE(3,400)Y(K)
20          GO TO 10
21        2 DE=E(K-1)-E(K)
22          ASF(K)=(SF(K)+SF(K-1))/2.
23          T=S-ASF(K)
24          DX(K)=DE/T
25          X(K)=X(K-1)+DX(K)
26          IF (K.EQ.N) WRITE (3,200) Q,Y(K), X(K), AN(J)
27       10 CONTINUE
28          GO TO 30
29      999 STOP
30      100 FORMAT (12F6.4)
31      200 FORMAT(F10.4,F10.3,F10.2,F10.4)
32      300 FORMAT 7X,'Q'6X,'DEPTH',6X,'DIST.',2X,'FRICTION
            FACTOR')
33      400 FORMAT(10XF10.3)
34      500 FORMAT(F10.3)
35      600 FORMAT(15)
36          END
```

VITA

Danny Lee Fread was born July 17, 1938, in Tuscola, Illinois. He graduated from Lovington High School in Lovington, Illinois, in 1956 and attended Carthage College from 1956 to 1959. He then attended the University of Missouri-Rolla, where he graduated in June 1961 with a degree of Bachelor of Science in Civil Engineering.

He accepted employment with Texaco Inc. as an Assistant Design Engineer at their petroleum refinery located in Lawrenceville, Illinois, where he remained until September 1967, during which time he was promoted to Senior Design Engineer and became a registered professional engineer in the state of Illinois.

In September 1967, he received a leave of absence to resume his studies at the University of Missouri-Rolla, where at the present time, having received a NDEA Title IV Fellowship, he is working toward the degree of Master of Science in Civil Engineering.